REPUBLIC OF TURKEY
ADANA ALPARSLAN TÜRKEŞ SCIENCE AND TECHNOLOGY UNIVERSITY

INSTITUTE OF GRADUATE STUDIES
DEPARTMENT OF MECHANICAL ENGINEERING

HEAT TRANSFER ANALYSIS OF HIGH HEAT FLUX MOVING SURFACE WITH NANOFLUIDS AND IMPINGING JETS

Mine EFEOĞLU

MASTER OF SCIENCE

ADANA 2021

REPUBLIC OF TURKEY

ADANA ALPARSLAN TÜRKEŞ SCIENCE AND TECHNOLOGY UNIVERSITY

INSTITUTE OF GRADUATE STUDIES

DEPARTMENT OF MECHANICAL ENGINEERING

HEAT TRANSFER ANALYSIS OF HIGH HEAT FLUX MOVING SURFACE WITH NANOFLUIDS AND IMPINGING JETS

Mine EFEOĞLU

MASTER OF SCIENCE

SUPERVISOR

Assoc. Prof. Dr. Mustafa KILIÇ

ADANA 2021

ABSTRACT

HEAT TRANSFER ANALYSIS OF HIGH HEAT FLUX MOVING SURFACE WITH NANOFLUIDS AND IMPINGING JETS

Mine EFEOĞLU

Department of Mechanical Engineering
Supervisor: Assoc. Prof. Dr. Mustafa KILIÇ

June 2021, 64 pages

In this study, the common effect of heat transfer from a high heat flux moving copper plate with the impinging fluid jet technique of nanofluids was examined numerically. In the first phase of the study, heat transfer analysis of as the basic fluid Cu-H_2O nanofluids in different Reynolds numbers and different particle diameters was performed on a stationary plate to confirm the current studies in the literature. The model results were compared and verified with existing experimental studies in the literature. In the second phase, heat transfer analysis was performed at different particle diameters, different plate velocity, and different volume ratios using Al_2O_3-H_2O nanofluid on both a moving and stationary plate. Furthermore, the effect of heat transfer was examined in the case of using different types of nanofluids in the moving copper plate. In the numerical study, the low Re numbered k-ε turbulence model of PHOENICS CFD program was used. This model is preferred because it is widely used in the modelling of confined impinging jets. According to the results of the study, if the number of Reynolds is increased to Re=12000-18000, the average number of Nusselts is increased by 28%, and when the nanoparticle diameter is reduced from D_p=40nm to 10nm, the average number of Nusselts increases by 9.1%, when the plate velocity was increased in the range of V_{plate}=0-6 m/s, the number of average Nusselts increased by 88.9%, the volumetric ratio is increased by 2.5% in the range of φ=0.5-2.0, and in case of comparing different nanofluids were compared, the best heat transfer performance was determined by Cu-H_2O nanofluid.

Keywords: CFD, heat transfer, impinging fluid jet, moving plate, nanofluid.

ÖZET

NANOAKIŞKAN VE ÇARPAN JETLER İLE YÜKSEK ISI AKILI HAREKETLİ BİR YÜZEYİN ISI TRANSFER ANALİZİ

Mine EFEOĞLU

Makina Mühendisliği Anabilim Dalı

Danışman: Doç. Dr. Mustafa KILIÇ

Haziran 2021, 64 sayfa

Bu çalışmada, yüksek ısı akılı hareketli bakır bir plakadan olan ısı transferinin, nanoakışkanların çarpan akışkan jet tekniği ile oluşturduğu müşterek etki sayısal olarak incelenmiştir. Çalışmanın ilk aşamasında, literatürdeki mevcut çalışmaları doğrulamak amacıyla temel akışkan olarak Cu-H_2O nanoakışkanın hareketsiz bir plakada farklı Reynolds sayılarında ve farklı parçacık çaplarnda ısı transfer analizi yapılmıştır. Model sonuçları literatürdeki mevcut deneysel çalışmalarla karşılaştırılmış ve doğrulanmıştır. İkinci aşamasında ise, hem hareketli hem de hareketsiz bir plakada Al_2O_3-H_2O nanoakışkanı kullanılarak farklı parçacık çaplarında, farklı plaka hızlarında, farklı hacim oranlarında ısı transfer analizi yapılmıştır. Ayrıca hareketli bakır plakada farklı tip nanoakışkan kullanılması durumunda ısı transferine olan etki de incelenmiştir. Sayısal çalışmada PHOENICS HAD programınn düşük Re sayılı k-ε türbülans modeli kullanılmıştır. Bu model, sınırlandırılmış çarpan jetlerin modellenmesinde yaygın bir şekilde kullanıldığı için tercih edilmiştir. Sonuç olarak; Reynoldas sayısının Re=12000-18000 değerine arttırılması durumunda ortalama Nusselt sayısında %28 oranında bir artış sağlandığı, nanoparçaçık çapı D_p=40nm'den 10nm'ye azaltığında ortalama Nusselt sayısında %9,1'lik artış sağlandığı, plaka hızı V_{plaka}=0-6 m/s aralığında arttırıldığında ortalama Nusselt sayısında %88,9 oranında artış sağlandığı, hacimsel oran φ=0,5-2,0 aralığında arttırıldığında ortalama Nusselt sayısında %2,5'lik artış sağlandığı, farklı nanoakışkanların karşılaştırılması durumunda ise, en iyi ısı transferi performansının Cu-H_2O nanoakışkanın gösterdiği belirlenmiştir.

Anahtar Kelimeler: çarpan akışkan jet, hareketli plaka, HAD, ısı transferi, nanoakışkan.

to my very dear family...

ACKNOWLEDGEMENTS

I would like to express my endless thanks to my invaluable teacher Assoc. Prof. Dr. Mustafa KILIÇ, who has never spared me his support during the planning, preparation and execution of my work during my thesis study, has guided me with his valuable knowledge and experience.

I would like to thank my teacher, Prof. Dr. Hakan ÖZTÜRK, who has always shown his support in my life and has been a light for me with his experiences.

I would like to thank my dear family who has shown their support in every period of my life and have made great contributions and efforts in my life.

TABLE OF CONTENTS

ABSTRACT iii
ÖZET iv
ACKNOWLEDGEMENTS vi
TABLE OF CONTENTS vii
LIST OF FIGURES ix
LIST OF TABLES xi
NOMENCLATURE xii
1. INTRODUCTION 1
1.1. Enhancement of Heat Transfer 1
1.2. Nanofluid 2
1.1.1. Nanoparticle Material and Base Fluid 4
1.1.2. Advantages of Nanoparticles over Microparticles 5
1.3. Thermophysical Properties of Nanofluids 6
1.3.1. Thermal Conductivity 7
1.3.2. Viscosity 10
1.3.3. Specific Heat 12
1.3.4. Density 13
1.5. Applications of Nanofluids 14
1.5.1. Transportation 14
1.5.2. Micromechanical Systems 14
1.5.3. Heating, Ventilating and Air-Conditioning (HVAC) Systems 15
1.5.4. Medicine 15
1.6. Impinging Jets 15
1.6.1 Single Impinging Jets 15
1.6.2. Multiple Impinging Jets 17
2. LITERATURE REVIEW 20
2.1. Literature Review on Nanofluids 20
2.2. Literature Review on Impinging Jets 24
3. MATERIALS AND METHODS 30
3.1. Model Geometry 30
3.2. Mathematical Formulation 34

3.3. Verification of Numerical Results 36
4. RESULTS AND DISCUSSION 39
4.1. Effect to Heat Transfer at Different Reynolds Numbers of Cu-H_2O Nanofluid 39
4.2. Effect to Heat Transfer at Different Particle Diameters of Cu-H_2O Nanofluid 42
4.3. Effect to Heat Transfer at Different Particle Diameters of Al_2O_3-H_2O Nanofluid 45
4.4. Effect to Heat Transfer at Different Plate Velocities of Al_2O_3-H_2O Nanofluid 47
4.5. Effect to Heat Transfer at Different Volume Ratios of Al_2O_3-H_2O Nanofluid 49
4.6. Effect to Heat Transfer of Different Types of Nanofluids 51
5. CONCLUSIONS 54
6. RECOMMENDATIONS 56
REFERENCES 57
App. 1. CFD flow diagram 64

LIST OF FIGURES

Figure 1.1. a) TEM image of an agglomerated nanoparticles TEM image of nanoparticles b) TEM image of dispersed nanoparticles 3
Figure 1.2. Comparison of nanoparticles with microparticles in heat transfer fluid 6
Figure 1.3. Comparison of thermophysical properties of nanofluids with pure water 7
Figure 1.4. Comparison of thermal conductivity for different materials 8
Figure 1.5. Comparison of with volumetric concentration of specific heat change of the nanofluids 12
Figure 1.6. Flow structure of a jet impacting vertical to a flat surface. 16
Figure 1.7. Interaction of multiple jets.. 17
Figure 1.8. a) Jet interaction, b) Jet split or fountain effect 18
Figure. 3.1. CFD Model Geometry. 32
Figure. 3.2. Mesh Structure... 32
Figure. 3.3. Comparison of the numerical model 34
Figure. 3.4. Independence of the mesh number. 37
Figure. 3.5. Independence from the iteration number. 37
Figure. 3.6. Comparison of model results with experimental results (φ = 1.5%) for Cu-H_2O nanofluid 38
Figure. 4.1. Change of local Nusselt number at different Reynolds numbers (dp=20 nm and φ= 4%) of the Cu-H_2O nanofluid. 40
Figure. 4.2. Temperature contours of Cu-H_2O nanofluid for a) Re=12000 and b) Re=18000 (dp =20 nm and φ=4%). 41
Figure. 4.3. Velocity vectors of Cu- H_2O nanofluid for a) Re=12000 and b) Re=18000 (dp=20 nm and φ= 4%)... 41
Figure. 4.4. Effect to local Nusselt number of different particle diameters.......................... 42
Figure. 4.5. Temperature contours of the Cu- H_2O nanofluid for a) D_p = 10 nm and b) D_p = 80 nm (Re = 16000 and φ = 4%)... 43
Figure. 4.6. Velocity vectors of the Cu- H_2O nanofluid for a)D_p=10nm and b)Dp=80nm (Re=16000 and φ=4%)... 44
Figure. 4.7. Effect to local Nusselt number of different particle diameters.......................... 45
Figure. 4.8. Effect to average Nusselt number of different particle diameters 46

Figure. 4.9. Plate temperature contours of Al_2O_3-H_2O nanofluid for a) D_p=10nm and b) D_p = 40nm. 46
Figure. 4.10. Effect to local Nusselt number of different plate velocity..... 47
Figure. 4.11. Effect to average Nusselt number of different plate velocity..... 48
Figure. 4.12. Plate Temperature contours of Al_2O_3-H_2O nanofluid for a)V_{plate}=0 m/s and b) V_{plate} = 6 m/s..... 49
Figure. 4.13. Local Nusselt numbers at different volume ratios..... 50
Figure. 4.14. Average Nusselt numbers at different volume ratios 50
Figure. 4.15. Plate temperature contours of Al_2O_3-H_2O nanofluid for a) ϕ=0.5 and b) ϕ=2.0...... 51
Figure. 4.16. The effect on the local Nusselt number of different nanofluids...... 52
Figure. 4.17. The effect on the average Nusselt number of different nanofluids 52
Figure. 4.18. Plate Temperature contours a) Pure water b) Cu-H_2O. 53

LIST OF TABLES

Table 1.1. Thermal conductivity of different materials. 5
Table 3.1. Boundary Conditions. 33
Table 4.1. Thermophysical properties of nanofluids at 20ºC. 51

NOMENCLATURE

Al_2O_3	: Aluminum Oxide
CuO	: Copper Oxide
TEM	: Transmission Electron Microscope
Cu	: Copper
Ag	: Silver
Ni	: Nickel
Au	: Gold
MgO	: Magnesium Oxide
ZnO	: Zinc Oxide
SiO_2	: Silicon Dioxide
Fe_2O_3	: Iron (III) Oxide
TiO_2	: Titanium Dioxide
SiC	: Silicon Carbide
AlN	: Aluminum Nitride
CNT	: Carbon Nanotube
MWCNT	: Multiwalled Carbon Nanotube
EG	: Ethylene Glycol
PG	: Propylene Glycol
k	: Heat conduction coefficient (W/m)
ρ	: Density (kg/m^3)
μ	: Dynamic viscosity (Pa.s)
C_p	: Specific heat (J/kgK)
k_f	: Heat conduction coefficient of the base fluid
k_p	: Heat conduction coefficient of nanoparticle
k_{nf}	: Heat conduction coefficient of nanofluid
ϕ	: Volume Ratio
ϕ	: Volume Ratio
β	: Layer thickness
Re	: Reynolds Number ($Re = V.\rho.Dh / \mu$)
Pr	: Number of Prandtl ($Pr = \mu.Cp / k$)
T	: Temperature (°C)

T_{fr}	: Freezing Point of Basic Fluid (℃)
T_j	: Jet inlet temperature (℃)
μ_{eff}	: Effective viscosity of the nanofluid
μ_{bf}	: Viscosity of the base fluid
μ_{nf}	: Viscosity of nanofluid
φ	: Volume ratio
$C_{p,nf}$	: Specific heat of nanofluid
$C_{p,np}$	: Specific heat of the nanoparticle
$C_{p,bf}$	: Specific heat of the base fluid
$C_{p,p}$	: Specific heat of the particle
$C_{p,bf}$	: Specific heat of the base fluid
ρ_{nf}	: Nanofluid density
ρ_{bf}	: Density of the base fluid
ρ_{np}	: Nanoparticle density
D_p	: Nanoparticle diameter
nm	: Nanometer (1 nm =10^{-9} m)
µm	: Micrometer (1 µm =10^{-6} m)
q''	: Heat Flux (W/m^2)
$q''_{surface}$	: The heat flux at the surface (W/m^2)
Nu	: Nusselt number (Nu = Q.Dh / ΔT.k)
T_s	: Surface temperature
D_h	: Hydraulic diameter
V_{jet}	: Jet outlet velocity (m/s)
V_{plate}	: Plate velocity (m/s)
Nu_{avg}	: Average Nusselt number
H	: Channel height (m)
D	: Jet diameter (m)
H/D	: The ratio of channel height to jet diameter
h	: Heat convection coefficient (W/m^2 K)
A	: Convection surface area (m^2)
$Re_{(p)}$	: Reynolds number of the nanoparticle
d_p	: Nanoparticle diameter (nm)
T_{inlet}	: Jet inlet temperature (℃)

L	: Plate length (m)
U	: Velocity component in X direction (m/s)
V	: Velocity component in Y direction (m/s)
W	: Velocity component in Z direction (m/s)
HAD	: Computational Fluid Dynamics
CFD	: Computational Fluid Dynamics
ε	: Kinetic energy absorption of turbulent flow

1. INTRODUCTION

1.1. Enhancement of Heat Transfer

Nowadays, the rapid improvement of technology requires the construction of more complex electronic devices. This situation increases the thermal loads of electronic circuit elements and the increased thermal load affects the service life of electronic devices. The most important issue affecting service life is whether the electronic chip can distribute heat quickly and efficiently. Thus, heat transfer is very significant in the cooling of electronic circuit elements. In industrial applications, overheating of the system is the most important factor that causes system failures and it reduces the efficiency of the system. Therefore, the heat transfer from the system is very important for the system to work efficiently and safely in industrial applications (Sun et al., 2019). For instance, in order to maintain the heat in the vehicles which are produced by the main carrier, the heat must be removed from the system. Similarly, a cooling system is needed for electronic devices to dissipate heat. Heat transfer processes are required in heating, ventilation and air-conditioning (HVAC) systems. Besides these; in many production processes, it involves heat transfer process in different ways, such as cooling a machine tool, pasteurizing food or setting the temperature to trigger a chemical process. In such application heat transfer process is provided by heat transfer equipment such as heat exchangers, evaporators, condensers and heat absorbers. Thus, by increasing the heat transfer efficiency of such equipment, the area covered by the device is minimized and so more compact equipment can be obtained (Özerinç 2010).

Heat transfer coefficient *(h)* is used to compare and evaluate the efficiency of fluids. The heat transfer coefficient of a liquid of a certain temperature, flow rate and pipe diameter; thermal conductivity (k), density (ρ), viscosity (μ), and specific temperature (C_p) can be calculated. A fluid with a significant heat transfer coefficient can allow for a reduction in system sizing, increased production output and reduced energy costs (Timofeeva et al., 2011).

It is possible to increase heat transfer by increasing surface area, using vibration and micro-channels. The efficiency of heat transfer is also carried out by increasing the thermal conductivity of the fluid. Conventional heat transfer fluids such as water, ethylene glycol and engine oil have low thermal conductivity. The thermal conductivity of solids is higher than liquids. Thus, the thermal conductivity of the liquid can be increased by adding solid particles to the liquids (Wang et al., 2003; Keblinski et al., 2002).

In recent years, nanofluids were started to enhance the heat transfer properties of the fluid. Nanofluids are created by adding nano-sized solid particles to the basic fluid. The heat conduction coefficient of this new mixture is quite high according to conventional heat transfer fluids. One of the important points of using nanoparticles is that nanoparticles make changes in the physical properties of single-phase liquid, such as density, viscosity and thermal conductivity, and it has a higher thermal conductivity than that of a single-phase liquid. Using conventional heat transfer fluids with low heat conduction coefficients in high heat flux applications is very difficult in terms of both the size and cost of the application. Therefore, it is foreseeable that nanofluids may be used in the future to replace conventional heat transfer fluids. Another method used to increase heat transfer is the jet cooling technique, which is one of the techniques that provide high cooling in the industry. The jet cooling technique intensifies the fluid at a certain place, minimizing the thermal boundary layer in that area. Thus, it provides high heat transfer in that area (Kilic 2013; Kakac and Pramuanjaroenkij, 2009).

1.2. Nanofluid

The term nanofluid was first used by Stephen Choi and J. Eastman at Argonne National Laboratory in 1995, they created suspensions containing nanometer-sized solid particles into the heat transfer fluid. Choi et al. added nanoparticles into water, ethylene glycol, and machine oil studied the effect of nanoparticles on the thermal conductivity. They found that the thermal conductivity of the liquid was higher than the base liquid after the nanoparticle was added (Choi and Eastman 1995; Aytac, 2020). Nanofluids are diluted suspensions of nanoparticles with a particle diameter less than 100 nm and these are considered a new solid-liquid mixture. These next-generation mixtures have high stability, high thermal conductivity, and heat transfer performance (Etaig 2017). Figure 1.1 shows TEM (Transmission electron microscope) images of Al_2O_3 and CuO nanoparticles of different particle sizes.

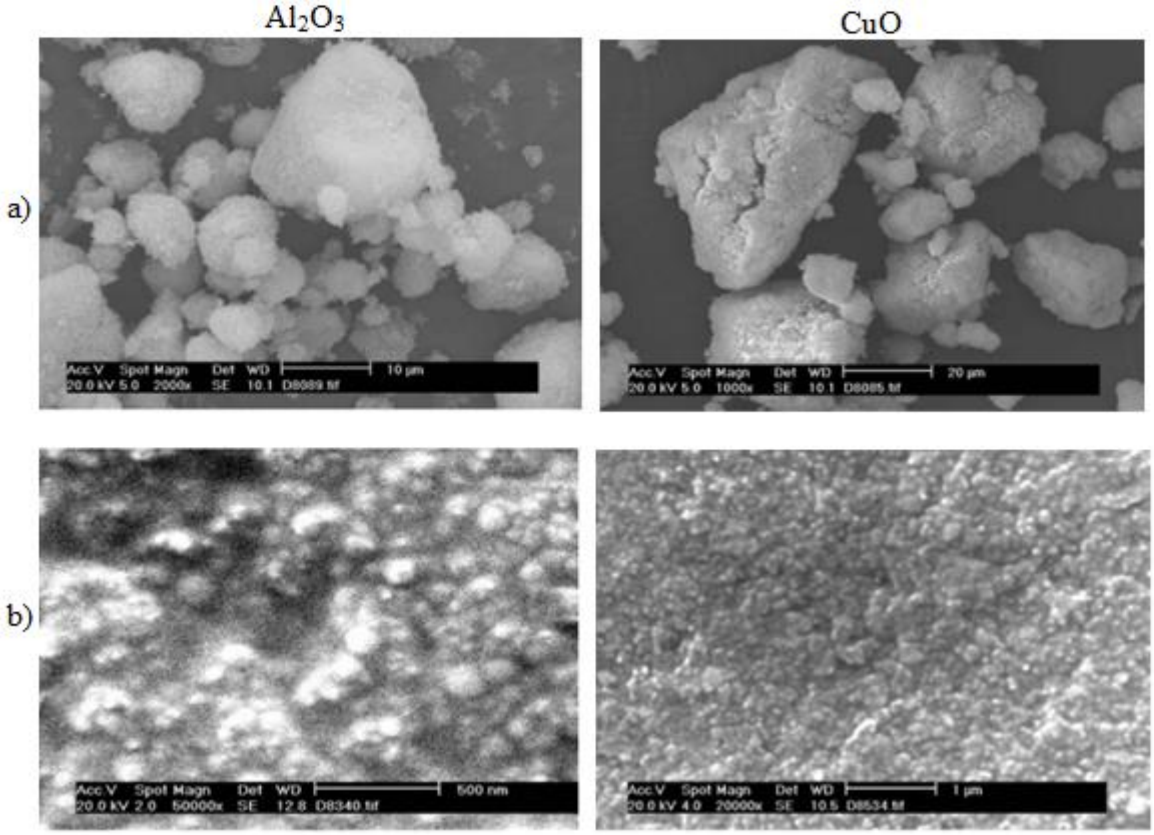

Figure 1.1. a) TEM image of an agglomerated nanoparticles TEM image of nanoparticles b) TEM image of dispersed nanoparticles (Putra et al.2003).

If we list the main properties of nanofluids:

- The most crucial properties of nanofluids are high thermal conductivity.
- More viscosity than base fluid.
- Stability. Nanoparticles are lightweight because they are very small, so they are less sedimentation. In studies, it has been reported that nanofluids maintain their stability for months using stabilizer material.
- Microchannel clogging without obstruction. Nanofluids are ideal not only for heat transfer applications but also for microchannel applications where high heat loads are needed. The combination of microchannel and nanofluid provides a high proportion of conductive fluid and a large heat transfer area. Microparticles in microchannels cannot be applied in this way because they obstruct the canals.
- Nanoparticles are very small and the acceleration to the wall is very small. This property reduces the chance of corrosion heat exchangers, pipelines and pumps.
- In the case of nanofluids are used, pumping power is reduced.
- Nanofluids can reduce effectively friction coefficient.

- In the case of nanofluid is used, it will save significant costs and energy so that heat exchanger systems are produced smaller and lighter.
- Nanofluid use provides more efficient flow lubrication, cooling and heating (Goharshadi et al., 2013).

The insufficiency of traditional heat transfer fluids to perform at increased thermal loads and in various thermal systems has led researchers, scientists and engineers to look for fluids with better heat transfer properties. Therefore, the use of nanofluids has become greatly important for improving the thermophysical properties of the fluid (Murshed et al., 2005). Nanofluids are quite important for different engineering applications that, necessary high heat spreading rates such as, cooling electrical components that require high heat generation, heat exchangers (Abdelrehim et al., 2019).

1.1.1. Nanoparticle Material and Base Fluid

Nanoparticles frequently used in nanofluid preparation can be grouped into:

- Metal particles (Cu, Ag, Ni, Au),
- Metal oxides (Al_2O_3, CuO, MgO, ZnO, SiO_2, Fe_2O_3, TiO_2),
- Metal carbide (SiC),
- Metal nitrure (AlN) and
- Carbon materials (CNT, MWCNT's, diamonds, graphite, fullerene) (Sajid et al., 2018).

Some metallic particles such as copper, aluminum, and zinc provide high thermal conductivity, but these metallic nanoparticles are limited in nanofluid applications due to their high reactivity and low stability. Non-metallic nanoparticles such as alumina (Al_2O_3) have lower thermal conductivity than metallic nanoparticles, and such particles have preferred properties such as high stability and chemical inertia. On the other hand, carbon nanotubes have many unique properties such as very high electrical and thermal conductivity, chemical stability, mechanical resistance, physical strength (Sarkar et al., 2015).

Basic fluids used in the preparation of nanofluids are traditional heat transfer fluids with low heat conduction coefficients such as water (H_2O), motor oil (EO), ethylene glycol (EG), propylene glycol (PG), and their mixtures (H_2O-EG, EG-PG) etc. Table 1.1 shows the values of thermal conductivity of different types of materials.

Table 1.1. Thermal conductivity of different materials (Kakaç and Pramuanjaroenkij, 2009).

Solids/liquids	**Material**	**Thermal conductivity (W/mK)**
Metallic solids	Silver	429
	Copper	401
	Aluminum	237
Nonmetallic solids	Diamond	3300
	Carbon nanotubes	3000
	Silicon	148
	Alumina(Al_2O_3)	40
Metallic liquids	Sodium (at 644 K)	72.3
Nonmetallic liquids	Water	0.613
	Ethylene glycol (EG)	0.253
	Engine oil (EO)	0.145

1.1.2. Advantages of Nanoparticles over Microparticles

Since heat transfer will occur on the surface of particles, it is possible to increase heat transfer by using particles with a larger surface area. At the same volumetric concentration, nanoparticles have a wider surface area than microparticles, which significantly increases heat transfer. In addition, nanoparticles transport about 20% of their atoms on their surface, the case makes them ready for heat conduction (Mursed et al.2008).

While some improvement in heat transfer was achieved when using micro dimension (1µm $=10^{-6}$m) particles, some significant disadvantages affecting the stability of the fluid (channel clogging, erosion of flow channels, rapid sedimentation and collection of particles, pump damage, etc.) could not be eliminated. Because the nanoparticles are so small, the effect of gravity on the nanoparticle is negligible, so the sedimentation is less and the nanofluid becomes more stable. Therefore, while microparticles were collapse in a short time, nanoparticles were very stable. Figure 1.2 shows the comparison of nanoparticles with microparticles in heat transfer fluids (Mursed et al.2008; Elçioglu 2013).

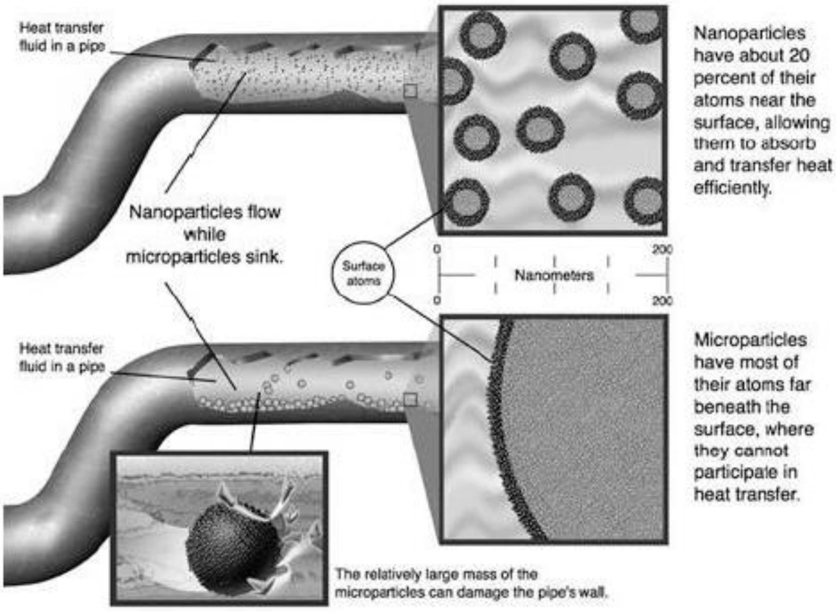

Figure 1.2. Comparison of nanoparticles with microparticles in heat transfer fluid (Elçioğlu, 2013).

1.3. Thermophysical Properties of Nanofluids

Understanding the thermophysical properties of nanofluids is considerable when using them in practical applications. It is necessary to determine the thermophysical properties of the prepared nanofluids before they can be used for system performance. Nanoparticle concentration has an effect on physical properties. As the particle concentration increases, the thermal conductivity, density, and viscosity of the nanofluids increase according to the base fluid, the specific heat value decreases. Figure 1.3 provided dimensionless physical properties of Al_2O_3 nanoparticle concentration compared to pure water (Sudarmadji et al. 2018).

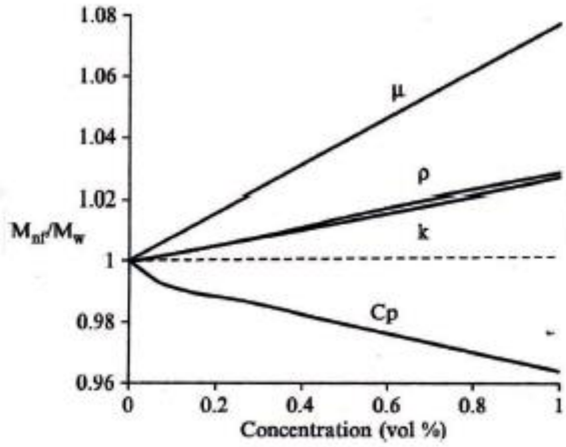

Figure 1.3. Comparison of thermophysical properties of nanofluids with pure water (Sudarmadji et al., 2018).

1.3.1. Thermal Conductivity

The capacity of the fluid or particle to conduction heat in the hot zone to the colder zone is defined as thermal conductivity. Nanofluids have quite high heat transfer properties than conventional heat transfer fluids. This is because suspended nanoparticles significantly increase the thermal conductivity of nanofluids. Reasons for this increase:

- Nanoparticles suspended in the liquid increase the surface area and heat capacity of the liquid.
- Suspended nanoparticles increase the effective thermal conductivity of the liquid.
- The interaction and impact motion between particles is intensified.
- Mixture fluctuation and turbulence density of the fluid increased.
- The dispersion of nanoparticles flattened the fluid's horizontal temperature gradient.

Thermal conductivity value of nanofluids in heat transfer applications varies depending on some parameters such as base fluid, nanoparticle shape, particle size, stability, temperature, pH value, particle materials, Brownian motion of nanoparticles, agglomeration effect of nanoparticles, distribution technique of nanoparticles, etc. (Xuan and Li, 2000; Kumar et al., 2015). Figure 1.4 shows thermal conductivity values for different materials.

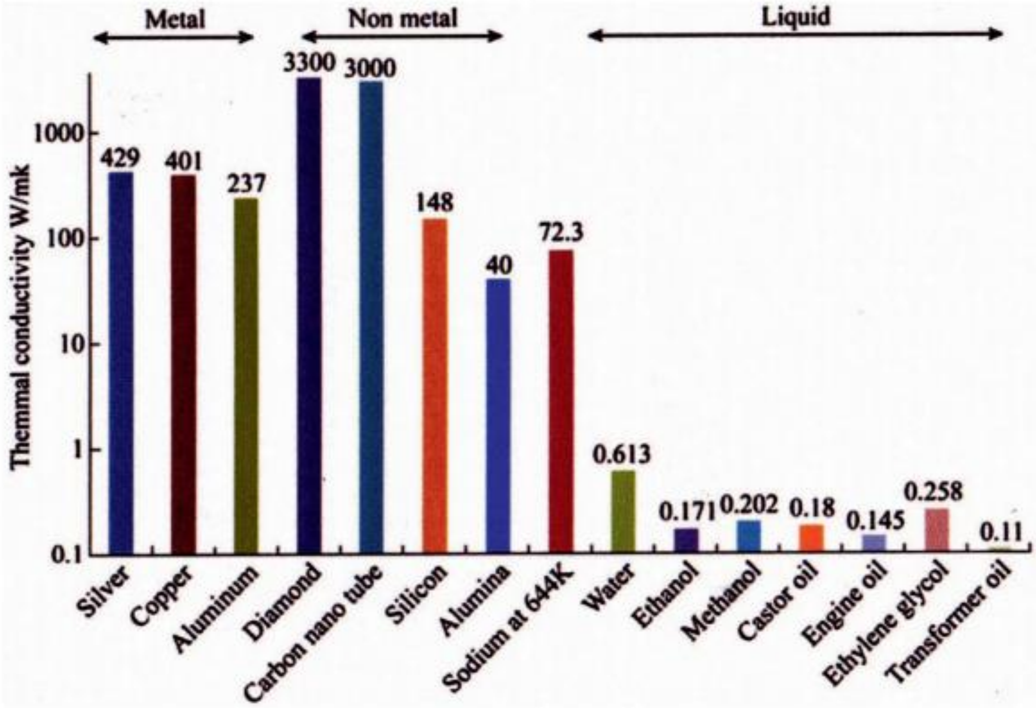

Figure 1.4. Comparison of thermal conductivity for different materials (Sudarmadji et al. 2018).

Considering the literature, various correlations have been developed by researchers to calculate the thermal conductivity values of nanofluids. The thermal conductivity model created by Maxwell in 1881 is suitable for spherical nanoparticles and the Maxwell model is recommended for large particle solid-liquid mixtures.

Maxwell model,
$$\frac{k_{eff}}{k_f} = \frac{k_p + 2k_f + 2\phi(k_p - k_f)}{k_p + 2k_f - \phi(k_p - k_f)} \tag{1.1}$$

According to the Maxwell model, the thermal conductivity of nanofluids depends on the base fluid, nanoparticle shape and volumetric concentration. As shown here, k_p is the thermal conduction coefficient of nanoparticles, k_f is the thermal conduction coefficient of the base fluid, ϕ is the volumetric ratio (Goharshadi et al., 2013; Kumar et al., 2015).

Theoretical models developed to determine the thermal conductivity values of nanofluids:

Bruggeman model,
$$\frac{k_{eff}}{k_f} = \frac{1}{4}\left[\left(3\Phi - 1\right)\frac{k_p}{k_f} + \left(2 - 3\Phi\right) + \frac{k_f}{4}\sqrt{\Delta} \right] \tag{1.2}$$

$$\Delta = \left[\left[(3\Phi-1)^2\left(\frac{k_p}{k_f}\right)^2 + (2-3\Phi)^2 + 2\left(2+9\Phi-9\Phi^2\right)\left(\frac{k_p}{k_f}\right)\right]\right] \quad (1.3)$$

The Bruggeman model is suitable for a two-phase mixture containing homogeneous spherical particles.

Hamilton– Crosser, $$\frac{k_{eff}}{k_f} = \frac{k_p + (n-1)k_f - (n-1)\Phi(k_f - k_p)}{k_p + (n-1)k_f + \Phi\left(k_f - k_p\right)} \quad (1.4)$$

The Hamilton-Croser model was developed using the shape factor. It is suitable for spherical and cylindrical particles. n=3 is taken. As seen here, k_f is the thermal conduction coefficient of the base fluid, k_p is the thermal conduction coefficient of nanoparticles, Φ is the volumetric ratio.

Wasp model, $$\frac{k_{eff}}{k_f} = \frac{k_p + 2k_f - 2\Phi(k_f - k_p)}{k_f + 2k_f + \Phi\left(k_f - k_p\right)} \quad (1.5)$$

The Wasp model has been suggested to calculate the thermal conductivity of solid-liquid mixtures. This model is not suitable for spherical nanoparticles.

Yu and Choi, $$\frac{k_{eff}}{k_f} = \frac{k_{pe} + 2k_f + 2\Phi\left(k_{pe} - k_f\right)(1+\beta)^3}{k_{pe} + 2k_f - \Phi\left(k_p - k_f\right)(1+\beta)^3} \quad (1.6)$$

The Yu and Choi model is another theory for calculating the thermal conductions of two-phase mixtures. In this model, the containment of the interfacial layer is based on the principle of parallel and series thermal conductivity overlap. β is the layer thickness and β= 1. As seen here, k_{pe} is the equivalent thermal conductivity, k_f is the thermal conduction coefficient of the base fluid, ϕ is the volumetric ratio, k_p is the thermal conduction coefficient of the nanoparticles (Kumar et al., 2015).

Within the scope of this thesis, the model used for the thermal conductivity calculation of nanofluid is explained below.

$$\frac{k_{eff}}{k_f} = 1 + 4.4\,\mathrm{Re}_{(p)}{}^{0.4}\,\mathrm{Pr}^{0.66}\left(\frac{T}{T_{fr}}\right)^{10}\left(\frac{k_p}{k_f}\right)^{0.03}\varphi^{0.66} \tag{1.7}$$

$\mathrm{Re}_{(p)}$ is the nanoparticle Reynolds number $\left(Re = \dfrac{2\rho_f k_b T}{\pi\mu_f{}^2 d_p}\right)$

As shown here, Pr is the Prandtl number of the base fluid, T is the temperature of the nanofluid (K), and T_{fr} is the freezing point of the base fluid, k_p is the thermal conduction coefficient of nanoparticles, k_f is the thermal conduction coefficient of base fluid, φ is the particle volume ratio. This equation is preferred because of the includes the basic fluid, nanoparticle heat transfer coefficients, particle diameter, nanoparticle volume ratio, density values, and nanoparticle dynamic viscosity in the calculation of nanofluid effective heat transfer coefficient (Corcione, 2011).

1.3.2. Viscosity

Another significant property of nanofluids is viscosity. Viscosity is a criterion for fluid friction and it is the fluid's resistance to flow. Changes occur in the viscosity values of the liquid by adding nanoparticles to the base fluid. Changes in viscosity have an important role in pumping power because the higher the viscosity, the greater the power necessary for pumping so, increasing the energy consumption of the pump. Temperature, nanoparticle concentration, nanoparticle size and shape, shear stress, surfactant addition, type of base fluid, etc. parameters affect viscosity (Pordanjani et al. 2018).

Viscosity models of nanofluids have been modelled as a function of volumetric concentration in the literature. The first of these models was proposed by Einstein in 1906 and it was modelled for spherical particles in very small volumetric proportions (less than 5%) (Dirlik 2018).

Theoretical models developed to determine the viscosity values of nanofluids:

Einstein (1906), $$\frac{\mu_{eff}}{\mu_{bf}} = 1 + 2.5\varphi \tag{1.8}$$

As seen in the equaiton, respectively, μ_{eff} is the effective viscosity of the nanofluid, μ_{bf} is base fluid viscosity, φ is the volume ratio of particles in suspension. The Einstein Model (Einstein, 1906) gives more accurate results for lower values of particle volumetric concentration. In the model, there is an assumption that the particles are spherical and there isn't an interaction between them.

Brinkman (1952), $$\frac{\mu_{eff}}{\mu_{bf}} = \frac{1}{(1-\varphi)^{2.5}} \tag{1.9}$$

It is the Einstein Model adapted to medium magnitude particle volumetric concentrations.

Batchelor (1977), $$\frac{\mu_{eff}}{\mu_{bf}} = 1 + 2.5\varphi + 6.5\varphi^2 \tag{1.10}$$

It is the extended version of the Einstein Model by taking into account the Brownian motion of particles.

Masoumi et al. (2009), $$\mu_{nf} = \mu_{bf} + \frac{\rho_p V_B d_p^2}{72C\delta} \tag{1.11}$$

$$C = \mu_{bf}^{-1}\left[(c_1 d_p + c_2)\varphi + (c_3 d_p + c_4)\right] \tag{1.12}$$

C is the correction coefficient. The values of the coefficients used in the calculation of this term are given as follows:

$c_1 = -1.133x10^{-6}, c_2 = -2.771x10^{-6}, c_3 = 9\,x10^{-8}, c_4 = -3.93x10^{-7}$

Within the scope of this thesis is explained below the model used for the viscosity calculation of nanofluid.

$$\mu_{nf} = \mu_{bf}(1+2.5\varphi+4.698\varphi^2) \tag{1.13}$$

As shown here, μ_{bf} is the dynamic viscosity of the base fluid. φ is the volumetric ratio of nanofluids (Elçioğlu et al.,2013; Batchelor 1977).

1.3.3. Specific Heat

Specific heat is a very important property that affects the heat transfer rate of the nanofluid. According to the current studies in the literature, the inclusion of nanoparticles causes a reduction in the specific heat of nanofluids in most cases (Pordanjani et al.2018). The specific heat change of nanofluids in the literature is given depending on the volumetric concentration in Figure 1.5.

For instance, as the volumetric concentration of water-based Al_2O_3, SiO_2, and CuO nanofluids increases, the change in specific heat decreases to -50%. On the other hand, molten salt-based Al_2O_3, SiO_2, TiO_2, and MWCNTs nanofluids occur at low volumetric concentrations of minimum - 20% and maximum 130% specific heat change. Specific heat values of nanofluids changes according to the nanoparticle type and volumetric concentration (Öcal, 2019).

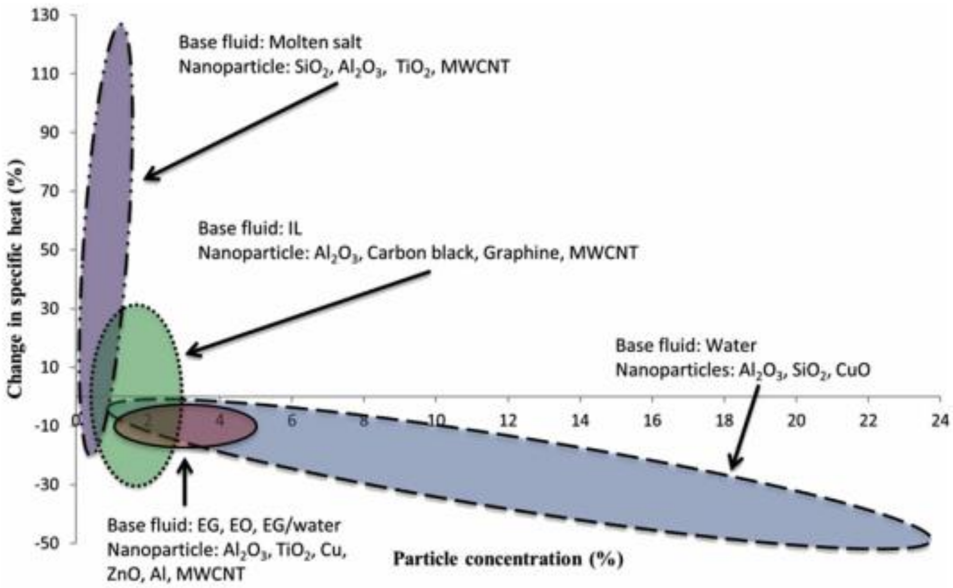

Figure 1.5. Comparison of with volumetric concentration of specific heat change of the nanofluids (Riazi et al., 2016).

Widely used theoretical models developed to calculate specific heat values of nanofluids:

Pak and Cho (1998) $$Cp,_{nf} = \left(Cp,_{np}\right)\varphi + Cp,_{bf}\left(1-\varphi\right) \tag{1.14}$$

As seen here, $Cp,_{nf}$ is the thermal capacity of the nanofluid, $Cp,_{np}$ is the thermal capacity of the nanoparticle, $Cp,_{bf}$ is the thermal capacity of base fluid, φ is the volumetric concentration.

Xuan and Roetzel (2000) $$\left(\rho C_p\right) = (1-\varphi)(\rho C_p)_{bf} + \varphi \tag{1.15}$$

$$\rho_{nf} = (1-\varphi)\rho_{bf} + \varphi\rho_{np} \tag{1.16}$$

As seen here, (ρCp) refers to the specific heat capacity, φ is the volumetric concentration (Pordanjani et.al., 2018).

Within the scope of this thesis, the equation proposed by the model Xuan and Roetzel used for the specific heat calculation of the nanofluid was used and is explained below.

$$Cp_{nf} = \frac{\varphi(\rho.C_p)_p + (1-\varphi)(\rho.C_p)_f}{\rho_{nf}} \tag{1.17}$$

As shown here $C_{p(p)}$ is the specific heat of the nanoparticle, $C_{p(f)}$ is the specific heat of the base fluid, and ρ_{nf} is the density of the nanofluid (Wang et al., 2006).

1.3.4. Density

Another parameter that is very important in nanofluid studies is the density of such fluids. Density is the amount of substance per unit volume and it changes depending on the temperature. Density and specific heat capacity are important factors in improving convective heat transfer in nanofluids. The density of a nanofluid can found with the equation (ρnf) by suggested Pak and Cho, and in this thesis, the equation suggested by Pak and Cho were used for the density calculation of the nanofluid.

Pak and Cho $$\rho_{nf} = (1-\varphi)\rho_{bf} + \varphi\rho_{np} \tag{1.18}$$

In this equation, φ is the nanofluid volume concentration, ρ_{bf} is the density of the base fluid, and ρ_{np} is the nanoparticle density (Pak and Cho, 1998; Dirlik 2018).

1.5. Applications of Nanofluids

In many fields, nanofluids are widely used due to the advanced thermophysical properties of nanofluids. Nanofluids can be used in the following industries.

1.5.1. Transportation

The use of nanofluid will improve heating and cooling applications in vehicles. Nanofluids have higher thermal conductivity potential compared to conventional vehicle heat transfer fluids (such as coolants, engine oil). The design of smaller engines, radiators and other vehicle components with nanofluids will assist in the production of lighter vehicles with higher energy efficiency and less fuel consumption. Lighter vehicles can cover a distance further with the same amount of fuel. Therefore, it will cause lower emissions with less fuel consumption and thus reduce environmental pollution. For this reason, nanofluids can make a great contribution to vehicle systems (Mursed et al., 2008).

1.5.2. Micromechanical Systems

Microchannel applications have high thermal loads. Nanofluids, on the other hand, have high heat transfer properties. The use together of microchannels and nanofluids will supply both highly conductive fluids and a large heat transfer area. Microelectromechanical systems (MEMS) produce too much heat during operation. High power micro-mechanical systems do not work well with conventional coolers. Therefore, solid particles can be added to such coolers to increase thermal conductivity. However, micro-mechanical systems are very small. This situation causes blockages in the channel and therefore cannot be applied in practical cooling systems. Since nano-sized particles can flow in microchannels without clogging, nanofluids will be the suitable coolant in microchannel applications (Mursed et al., 2008).

1.5.3. Heating, Ventilating and Air-Conditioning (HVAC) Systems

Heat transfer will be increased by the use of nanofluids in heating, ventilation, and air conditioning systems (HVAC). By reducing the size of the cooling and HVAC units, the pumping of the cooler will become easier. Therefore, it will increase pump and energy efficiency while creating a cost-effective system at the same time (Mursed et al., 2008).

1.5.4. Medicine

Effective drug delivery can be made possible by using magnetic nanoparticles in body fluids (biofluids) for cancer treatment._Unlike side effects such as DNA damage caused by current radiation therapy, nanoparticles are stickier to cancer cells than normal cells due to their surface properties. The magnetic nanoparticles are excited by an AC magnetic field and so effective drug delivery can be made possible in body fluids. The future use of nanofluids for drug delivery in body fluids is a promising initiative for cancer therapy (Mursed et al., 2008).

1.6. Impinging Jets

1.6.1 Single Impinging Jets

The jet cooling technique is one of the optimum heat management techniques that provide high cooling in the industry. The impinging jet is caused by the impact of the fluid coming out of a ringlet or nozzle to the surface, and turbulent impinging jets are often used to increase heat/mass transfer. The turbulence level of the impinging jet, from the surface center the distance of the ringlet, and the ringlet angle are important parameters for maximum heat/mass transfer In addition, some parameters affect the heat transfer event when creating impinging jets. These are nozzles shape (single, multi-sequence, long, narrow, slit, two-dimensional, etc.), size, height, the distance between the ringlet, the velocity, temperature, density of the slammed fluid, the way it hits the surface (rotating, angled, oblique, steep, etc.).

Jet impact technique is used by intensifying heating, cooling or drying processes on a surface. For instance, the impinging jet technique is used in modern jet engine aircraft to cool turbine blades which are heated by burning gases with high temperatures, tempered glass sheets, dry textiles and paper products, and to cool electronic circuit elements. In addition, it is used in heat treatment of metals, in many engineering applications such as paint, food industry, for heating cooking purposes (Kilic 2013).

The factor that makes the jet impact technique attractive is providing high heat transfer on a limited surface. Thus, very high rates of heat transfer can be obtained with minimum flow. Especially, it provides high heat transfer locally on the surface to be cooled in small-sized systems. In the impact air-jet technique using in surface cooling, the air is sprayed on the surface to be cooled by pressure. For this purpose, ringlets or nozzles of various diameters are used. Air impinging the surface creates a high heat transfer coefficient on the surface. The jet impact is used to gain a high local heat transfer coefficient between the fluid and the surface, and it also provides energy savings due to significant increases in heat transfers. In general, impinging jets are sprayed from D-diameter circular or W-extensiveness rectangular nozzle at a certain velocity and temperature. The impinging jet a flat surface is divided into 3 zones. These are the free jet zone is the stop or stagnation point zone and the wall jet zone (Kılıç 2013; Elibol and Türkoğlu, 2017). The parts of the impacting jet are shown in Figure 1.6.

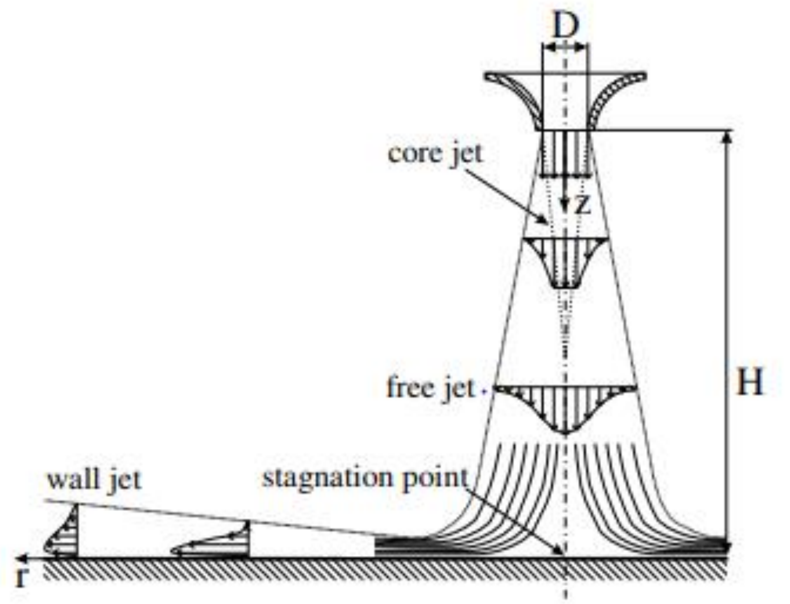

Figure 1.6. Flow structure of a jet impacting vertical to a flat surface (Hoffman et.al., 2007).

<u>In the Free Jet Zone</u>,

As the distance from the nozzle exit rises, the momentum transfer among the surrounding with the jet increases. This case causes the free boundary of the jet to expand gradually and constant velocity core to the contraction in a conical manner. Below the constant velocity core, the velocity is not constant across the entire jet section in the free jet zone, and the velocity decreases with distance from the nozzle outlet. With its general structure, this flow zone is defined as the "free jet zone".

Impact Zone (Stagnation Point),

The axis line of the jet is intersecting with the impact surface in jets that impact vertical to the target surface. At this point, the jet loses its axial velocity; this point is called the "stagnation point". The highest heat transfer occurs at the stagnation point.

Wall Jet Zone

This zone is accelerates again with the momentum transfer of fluid. The flow is affected from the target surface impact of the jet in the impact or stops zone. As a result of this, the velocity slows down in the vertical (y) direction and accelerates in the horizontal (x) direction (Elibol and Türkoğlu, 2017).

1.6.2. Multiple Impinging Jets

There are available many applications for single jet impact in the industry. In addition to this, the use of multiple jets a surface impact are also common. Multiple jets are used in many applications such as cooling of electronic equipment, cooling of turbine blades, and anti-icing systems in the aircraft industry (Medina 2008). Figure 1.7 shows the interaction of multiple jets.

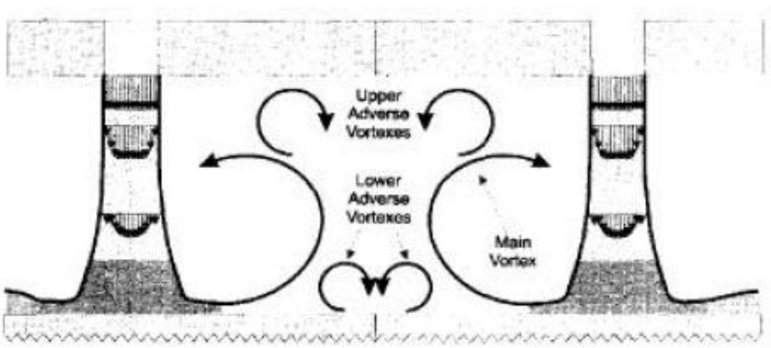

Figure 1.7. Interaction of multiple jets (Medina 2008).

In Figure 1.7, two reverse vortex zones were formed in the interaction between multiple jets. The fluid dynamics of a single jet collision is a complex issue, but the dynamics of multiple jets are more complex due to encounter and interaction. As a result, the performance of the single impact jet (on average Nu) is higher than the performance of multiple jets. Figure 1.8 shows jet combination and jet separation.

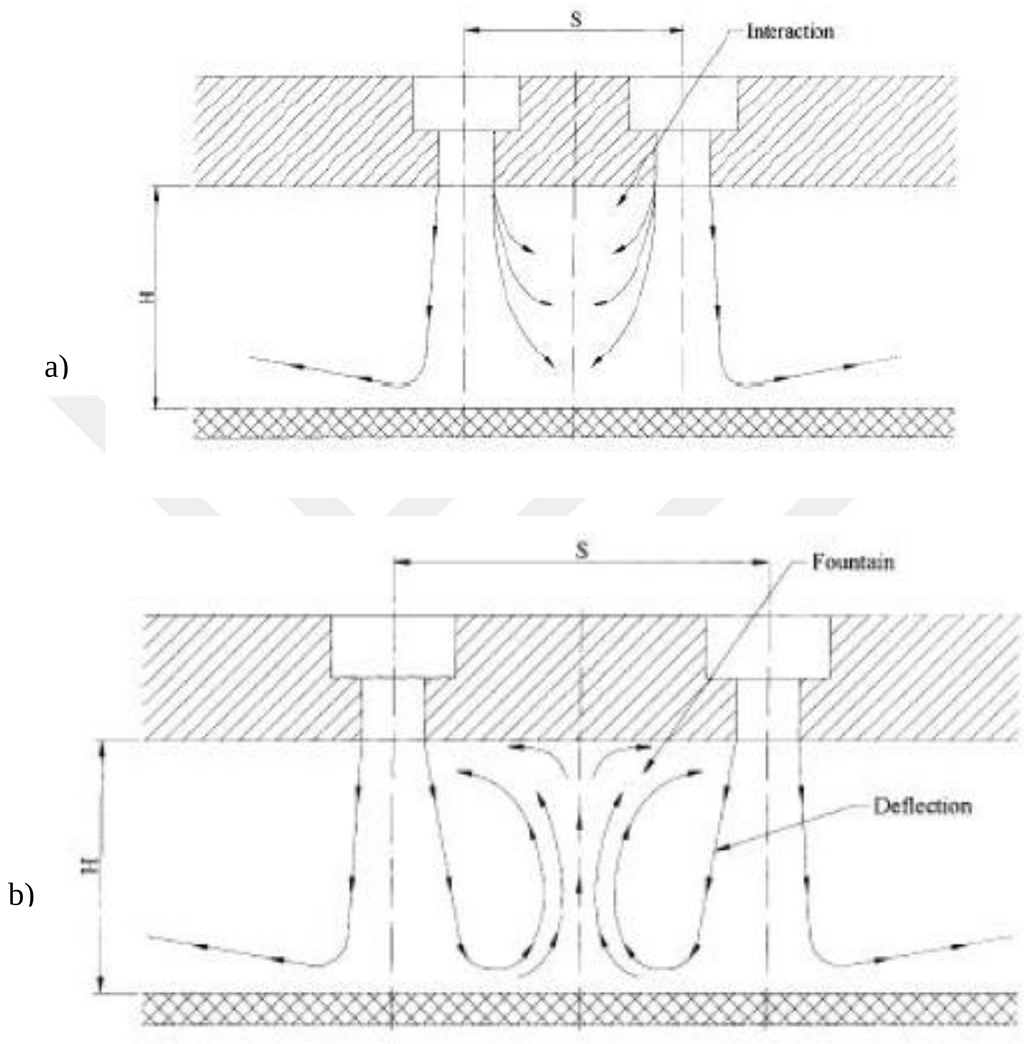

Figure 1.8. a) Jet interaction, b) Jet split or fountain effect (Medina 2008).

In Figure 1.8., two different types of interaction between multiple jets are defined. The jet interaction occurs before impact, this effect decreases the strength of the jet effect and, as a consequence, the overall heat transfer impairs. The jet split consists of an encounter of two adjacent wall jets. This situation continues cyclically between the fountain jet and the center jet. Consequently, the heat transfer of the jet array is impaired due to the drift effect (Medina 2008).

The aim of this thesis improves the heat transfer from a moving copper plate with high heat flux by using different types of nanofluid and impinging fluid jet technique. Thus, it was aimed to increase the heat transfer from the surface by planning to use the common effect of nanofluids in addition to the impinging jet technique.

PHOENICS CFD program was used for numerical analysis. In order to improve the heat transfer in the study, in accordance with the system geometry:

The effects on heat transfer has been studied of below elements:

- Different Reynolds numbers of Cu-H_2O nanofluid (Re= 12000,14000,16000,18000)
- Different particle diameters of Cu-H_2O nanofluid (D_p= 10nm, 20nm, 40nm, 80nm)
- Different particle diameters of Al_2O_3-H_2O nanofluid (D_p= 10nm, 20nm, 30nm, 40nm)
- Different plate velocities of Al_2O_3-H_2O nanofluid (V_{plate}= 0m/s, 2m/s, 4m/s, 6m/s)
- Volume ratios of Al_2O_3-H_2O nanofluid (φ= 0.5%, φ = 1%, φ = 1.5%, φ = 2%)
- The effect of heat transfer of different types of nanofluids (Cu-H_2O, Al_2O_3-H_2O, TiO_2-water) has been investigated.

In the current studies in the literature, there are some separately studies on the determination of the material characteristics of nanofluids and the effect on heat transfer of impinging jets. In this study; unlike the studies in the current literature, nanofluids were used with the impinging jet technique and it was aimed to investigate the effect of the common effect on heat transfer.

2. LITERATURE REVIEW

In this thesis, it is aimed to cool the surface of a moving copper plate with high heat flux by using the nanofluid and impinging jet effect together. Although there are separate studies on nanofluid and impinging jets in the literature, the number of studies in which the two effects are used together is very few. In this study, the literature research was examined in 2 stages.
In the first stage is studies examining the thermophysical properties of the fluid and the change in heat transfer in the case of using nanofluid. In the second stage, studies involving the change in heat transfer when using the nanofluid and impinging jet effect together were examined.

2.1. Literature Review on Nanofluids

Choi (1995) the idea of nanofluid was first proposed by Choi and stated that it improves heat transfer. Sarkar et al. (2015) and Kasaeian et al. (2015) conducted studies to identify the physical and thermal properties of nanofluids. Suresh et al. (2011) and Assef et al. (2014) the first engineering applications of nanofluids whose physical and thermal properties were determined. Selvakumar and Suresh (2012) cooling of electronic systems, Hadad et al. (2013) nuclear reactors, Devdatta et al. (2009) building heating and cooling systems, Ho et al. (2010) researches have been started to improve the heat transfer of nanofluids in many engineering applications such as boiling application.

Khan et al. (2021) compared experimentally the thermal conductivity of TiO_2/water mono nanofluid with TiO_2-Ag/water composite (hybrid) nanofluid. Different fluid temperatures (35°C, 40°C, 50°C, 60°C) and different volumetric concentrations (0.1, 0.2, 0.3, 0.4) are parameters examined in the study. According to this study, it was determined that the thermal conductivity fluids increased with the increase of nanofluid temperature and nanoparticle volumetric concentration, but the thermal conductivity of nanocomposite fluid was higher than that of mono nanofluid. A maximum improvement of 18.4% was achieved at 4% volumetric concentration and at 60°C for TiO_2/water nanofluid.

Peyghambarzadeh et al. (2011) analyzed the effect on heat transfer when adding pure water and pure ethylene glycol (EG) Al_2O_3 nanoparticle as the base fluid in the vehicle radiator. According to the results of the experimental, it has been stated that in the case of using nanofluid in base fluids, it provides an increase of approximately 40% compared to the base fluid.

Sundar et al. (2013) examined experimentally the thermal conductivity of the Fe_3O_4 magnetic nanoparticle and the nanofluid based on a mixture of Ethylene Glycol /Water. The mixture of ethylene glycol and water was studied in different base fluids such as 20:80%, 40:60% and 60:40% by weight. As a result; it was determined that thermal conductivity increased with the increase in particle concentration and temperature. The highest increase in thermal conductivity (at 2.0% particle volume concentration, at 60°C is 46% in 20: 80% EG/W based working fluid.

Nguyen et al. (2008) studied experimentally the effect of Al_2O_3-water nanofluid on dynamic viscosity. Two distinct particle sizes, 36 and 47 nm, were examined. As a consequently; it was determined that 36 and 47 nm Al_2O_3-water nanofluids at 4% particle volume concentration showed almost the same viscosity, but when the volumetric concentration was increased, 47 nm nanoparticulate nanofluids were found to have a higher viscosity value than the nanofluids formed with 36 nm particles.

Umer et al. (2015) examined the heat transfer from a surface at a different volumetric concentration by using CuO-water nanofluid. Consequently, it has been determined that as the particle volume concentration increases and the Reynolds number increases, the heat transfer coefficient also increases and the highest increment in the heat transfer coefficient is 61%.

Keblinski et al. (2002) researched the effect of nanoparticle sizes on thermal conductivity. They determined that as the particle diameter decreases, the thermal conductivity increases, but this increase cannot be explained by existing theories. 4 predictions have been identified to explain this situation. These are Brownian motion of the particles, the layering of the liquid at the liquid/particle interface at the molecular level, the nature of the heat transfer in nanoparticles and the nanoparticle aggregation effects. As a result, they determined that the key factor in understanding the thermal properties of nanofluids is ballistic, not diffusive.

Naraki et al. (2013) experimentally examined the change in heat transfer by using CuO-water nanofluid in a vehicle radiator. The effect of different volume ratios (0%-4%) of nanofluids has been investigated. As a result; it was determined that the heat transfer coefficient of nanofluid is higher than the base fluid. It was determined that as the volumetric ratio increased, the total heat transfer coefficient also increased, and as a result of increasing the volumetric concentration from 0% to 4%, there was an 8% increase in the total heat transfer coefficient.

Lee et al. (1999) measured the thermal conductivity value of the nanofluids formed with Al_2O_3 and CuO nanoparticles using the temporary hot wire method. The study is an experimental study. The experiments were compared with the Hamilton and Crosser model and it determined that the thermal conductivity for Al_2O_3-H_2O nanofluid can be predicted, but it is not compatible for nanofluids with CuO nanoparticles. Finally, they determined that thermal conductivity increases with the addition of nanoparticles and particle shape and size are important to increase the thermal conductivity of nanofluids.

Zhang et al. (2014) researched experimentally the heat transfer properties of TiO_2-water nanofluid in a multi and mini-channel straight tube. The parameters examined in the study are different nanoparticle diameters (dp=10, 30, 50 nm) and different volumetric ratios (0.005%-1%) of the TiO_2 nanoparticle. As a result; It was determined that as particle diameter (dp) increased, Nusselt number (Nu) decreased, but as the volumetric concentration increased, Nu number was not changed. In the case of particle diameter dp = 10 nm and volumetric concentration 0.01%, it has been determined provide an increase of 61% in the Nusselt number, which is the best heat transfer performance.

Wang et al. (2006) numerically investigated the behaviour of single-phase and multi-phase nanofluid at different Re numbers (Re = 2000-12000) for Cu-H_2O nanofluid. The addition of nanoparticles to the basic fluid considerably affects the fluid characteristics beyond increasing the heat conduction coefficient, therefore, turbulence models used for single-phase flow (k-ε, k-ω, RNG, etc.) cannot model the flow sufficiently, instead SST k-ϖ turbulence model, it was stated that multiphase models such as Eulerian-Eulerian turbulence model should be preferred.

Sun et al. (2020) experimentally investigated the effect of Fe_3O_4-water magnetic nanofluid on heat transfer. The effects of magnetic field gradient, magnetic flux density, and different magnetic field orientations to local Nusselt number were investigated. According to this study, it has been determined that rising the magnetic flux density and magnetic field gradient can provide a considerable development in convective heat transfer. Fe_3O_4-water nanofluid at 0.5% volumetric concentration provided an increase of 4.36% in the local Nusselt number. If the magnetic field is 700 Gauss, an increase of 7.19% was observed in the local Nusselt number. In addition, it has been determined that the reason for the increase in convective heat transfer is the emergence of a chain-like structure. Flow disorder caused by magnetic field has been determined to increase the pressure drop.

Lahari et al. (2018) studied the effect of different volumetric ratios (0.5%, 1.5%, 2.0%) of TiO_2-ZnO/water hybrid nanofluids on heat transfer in a double-pipe heat exchanger. According to the results of the experiment; the thermal conductivity of TiO_2 nanofluid has increased by 14.8% at 1.5% volumetric concentration compared to the water (base fluid) , and when the volumetric concentration is 2%, the thermal conductivity of volumetric concentration is 27.9%. The thermal conductivity of ZnO nanofluid has raised by 11.5% at 1.5% volumetric concentration compared to the water, and when the volumetric concentration is 2%, the thermal conductivity of volumetric concentration is 18.1%. It has shown significant improvement in both heat transfer rate and heat exchanger efficiency at the same volumetric ratios. It has been determined that the thermal conductivity and efficiency of the heat exchanger, TiO_2 and ZnO hybrid nanofluids increase 40.9% and 13.5% respectively at 1.5% volume ratio.

Nguyen et al. (2008) studied experimentally the effect of Al_2O_3-water nanofluid on dynamic viscosity. Two distinct particle sizes, 36 and 47 nm, were examined. As a consequently; it was determined that 36 and 47 nm Al_2O_3-water nanofluids at 4% particle volume concentration showed almost the same viscosity, but when the volumetric concentration was increased, 47 nm nanoparticulate nanofluids were found to have a higher viscosity value than the nanofluids formed with 36 nm particles.

Xuan and Li (2000) examined the impact of nanoparticle volume change, particle diameter and particle geometry on heat transfer for Cu-water nanofluid. It has been determined that if the volumetric ratio is increased from 2.5% to 7.5%, the nanofluid thermal conductivity coefficient increases from 1.24 to 1.78.

2.2. Literature Review on Impinging Jets

Teamah et al. (2015) researched the heat transfer and flow structure formed by the impact of Al_2O_3-water nanofluid against a flat plate numerically and experimentally at different Reynolds numbers (Re = 3000-32000) and nanofluid volume ratios (φ= 0-10%). As a result, as the volumetric ratio of nanoparticles in the fluid increased, heat transfer increased. This increase was found to be a 62% improvement compared to the base fluid. It was observed that if CuO-water nanofluid is used instead of Al_2O_3-water nanofluid, heat transfer can be increased by 8.9%, and if TiO_2-water nanofluid is used, an increase of 12% can be achieved.

Choo and Kim (2010) investigated the_impact of confined and unconfined impinging jets on heat transfer experimentally and numerically. Air and water are used as fluids. As a consequence, it has been determined that at constant pump power, the restricted jet flow performs similarly to the unrestricted jet flow.

Boudraa and Bessaïh (2020) numerically studied the flow and heat transfer effects of a hot cubic block exposed to turbulent flow using the impinging jet. The parameters examined in the study are the effect of Reynolds value (Re=1,1.5,2) on heat transfer, channel height and jet axis position._According to the result of the study; there is an increment in heat transfer with increasing Reynolds value and the best increase is Re=1 value. A decrease in the channel height significantly increased the heat transfer rate. When the position of the jet axis is towards the inlet of the channel, it has been observed that there is an increase in heat transfer.

Kilic and Ali (2019) investigated the heat transfer and flow properties when using nanofluids and multiple jets. As a result; when the nanofluid volumetric ratio was increased from ϕ=2% to ϕ=4%, the average Nusselt number increased by 10.4%. They determined that the positions of the multiple jets were effective in heat transfer and that the Cu-water nanofluid showed the best heat transfer performance.

Lv et al. (2017) Al_2O_3-water nanofluid has different volumetric ratios (0.5%, 1%, 1.5%, 2%) at different impact angles (ϴ =50º, 70º, 90º) and different Reynolds numbers (Re=5000-14000) has examined its effect experimentally. They found that Al_2O_3-water nanofluid could provide 61.4% enhancement in heat transfer compared to pure water with H/D_h=4, 2% volumetric ratio, Re=12000 value.

Kilic and Efeoglu (2019) examined the heat transfer change caused by the impact of the impinging fluid jet on a moving plate with high heat flux. Different types of nanofluids (Al_2O_3-H_2O, TiO_2-H_2O, pure water) and different volume ratios (φ = 0.5, 1.0, 1.5, 2.0) are the parameters studied in the study. According to the study, it was determined that as the nanofluid volumetric ratio increased, the average Nusselt number increased and the surface temperature decreased, but it was determined that this increase in the average Nusselt number continued as to decrease for increasing volumetric ratios. In the case of using different nanofluids, it was determined that the best heat transfer performance was Cu-H_2O nanofluid. In the event of using Cu-H_2O nanofluid; the average Nusselt number increased by 2.9% according to TiO_2-H_2O, 3.1% according to Al_2O_3-H_2O nanofluid and 7.7% according to pure water.

Sun et al. (2016) investigated the change in heat transfer of an impinging jet created with CuO nanofluid. As a result, it has been determined that when using nanofluid, a significant increase can be achieved in heat transfer compared to using only water. It has been found that there is no significant change in pressure drop. A higher heat transfer coefficient was obtained when a circular nozzle was used instead of a square-shaped nozzle. It has been determined that the highest heat transfer is obtained when the jet angle is 90º.

Kilic and Ozcan (2017) examined the effect on heat transfer when using multiple jets and different types nanofluids on a surface with high heat flux. As a result, they determined that the increment in the Re number and the reduction in the particle diameter caused an increase in heat transfer, and in the case of using Cu- H_2O nanofluid, an increase of 9.3% compared to Al_2O_3 -water nanofluid and 8.4% compared to TiO-water nanofluid could be achieved.

Dagtekin and Oztop (2007) investigated numerically the effect of double jet flow in isothermal walls on heat transfer in a laminar flow regime. The jet Reynolds numbers, the position on the wall of the jet fluids, and the distance of the jets to each other are parameters examined in the study. Air was used as fluid (Pr=0.71). As a result of the effect of two jets in the channel, a multi-layered flow occurred in the impact zone. The average Nusselt number increased linearly with increasing Reynolds number. It has been observed that heat transfer increases significantly when the Reynolds number of the first jet is greater than the second jet.

To sum up, It has been determined that as the two jets approach each other, the effect of the second jet decreases and behaves like a single jet.

Nguyen et al. (2009) experimentally investigated the heat transfer performance from a heated surface by using Al_2O_3-water nanofluid with a limited and submerged impact jet.Particle volumetric ratio and the distance of the jet from the heated surface for both laminar and turbulent flows are the parameters studied in the study. The nozzle diameter is 3 mm and the distance from the nozzle to the heated surface is between 2.5 and 10 mm, the particle volume ratio is between 0 and 6%. Consequently; it has been determined that if the particle volume ratio is 2.8% and the jet-surface distance is 5 mm, the highest surface heat transfer coefficient can be obtained.

Barewar et al. (2019) examined experimentally the heat transfer properties of ZnO-water nanofluid at different jet-plate surface distance (2-7.5) and different volume concentration (φ=0.02% - 0.1%) by impacting the heated copper plate surface. As a result; as the particle concentration increases, the heat transfer increases, and when the volumetric concentration is φ=0.1%, there is a 51% increase in heat transfer compared to pure water for the ZnO nanofluid. It has been determined that there is maximum improvement in heat transfer when the jet-plate distance H/D_h=3.5 at the nanofluid ϕ = 0.1% volumetric concentration.

Nayak et al. (2016) compared the thermal performances of Al_2O_3 and TiO_2 nanofluids and they investigated experimentally the effect of two impacting nanofluid jets at different volumetric ratios (0.01%, 0.03%, 0.05%, 0.07%) on heat transfer. As a consequence, it has been determined that these two different nanofluids show similar performance, the rise in heat transfer is due to the behaviour of the nano-particles in the flow rather than the increase in the heat transfer coefficient, so Al_2O_3-water nanofluid has a better performance than TiO_2-water nanofluid because it can provide a more homogeneous distribution.

Kilic et al. (2017) researched the cooling effect of a flat plate with constant heat flux with the help of an impinging air jet. Dimensionless channel heights and different Reynolds numbers are parameters investigated in the study. As a result, by increasing from Re=4000 to Re= 10000, the average Nusselt number increased in the range of 49.5%. It was determined that by increasing the jet plate distance between H/D_h = 4-10, an increase of 17.9% was achieved.

Kilic and Baskaya (2017) analyzed numerically the improvement of heat transfer on the surface with constant heat flux by using impinging fluid jet and flow baffler of different geometries together. In the study, the flow and heat transfer in the channel with and without flow diverter was investigated for different Reynolds numbers and the jet hydraulic diameter (H/D) ratios of the channel height. According to the results of the study, by using the impinging fluid jet and different geometry flow baffler together; it has been observed that an increase of up to 28% can be provided in heat transfer, depending on the case of not using flow baffler. Furthermore, it has been determined that the heat transfer increases with the increase in the Re number.

McGuinn et al. (2007) examined the heat transfer provided by the nozzle with two different outlet geometries (flat outlet and shaped). This study is numerical and experimental as an examined. As a consequence, it has been observed that the shaped nozzle provides a more effective heat transfer compared to the flat nozzle. It has been determined that the heat transfer on the surface is not only due to the turbulence that occurs but also to the geometry of the flow coming to the surface.

Kareem et al. (2019) investigated experimentally when using the CuO-water nanofluid with impinging jet technique, the hydrodynamic property of flow and its effect on heat transfer. Different Reynolds numbers (Re=1000-8000) and particle concentrations (φ =0.1–0.3) are the parameters examined in the study. Consequently, heat transfer increased as both particle volume ratio and Reynolds number increased. It was determined that increasing the distance between the nozzle-target plate caused the Nusselt number to decrease, and the maximum increase in Nusselt number was 2.9% and the minimum increase was 0.87.

Abdelrehim et al. (2019) numerically studied the heat transfer and flow analysis of a single impact jet. They investigated the effects of nanoparticle volume concentration (Ø=0-4%), Reynolds number (Re=100-400), and jet height ratio (H/W=0.5-4) and on local and mean Nusselt number. As a result, the Nusselt number increased as both Reynolds and volumetric concentration increased. If the volumetric ratio is = 4% and the jet height ratio is H/W = 4, a maximum increase of 150% in the average Nusselt number was found.

Kilic and Efeoglu (2019) investigated the effect of the joint effect of nanofluid and impinging jets on heat transfer by impacting a moving plate with high heat flux. Different nanofluid particle diameters (D_p=10, 20, 30, 40 nm) and different plate velocities (V_{plate}=0, 2, 4, 6 m/s) are the parameters examined in the study. Al_2O_3-H_2O nanofluid was used as the basic fluid in the study. Consequently; it was determined that as the particle diameter decreased, the average Nusselt number increased and the surface temperature decreased, and the best heat transfer performance was D_p =10 nm. It has been determined that as the plate velocity rises, the average Nusselt number increases, but this increase continues by decreasing as the plate velocity increases. The increase in Nu_{avg} in the range of V_{plate}=0-2 m/s was 40.9%, the increase in Nu_{avg} in the range of V_{plate}=2-4 m/s was 23.9%, and the increase in Nu_{avg} in the V_{plate}=4-6 m/s range was 8.1%.

Ersayın and Selimefendigil (2013) investigated the heat transfer and flow properties of vibrating and non-vibrating flow of the impinging jet formed for Al_2O_3-water nanofluid on a moving plate. In numerical simulation, nanoparticle volume ratio (φ=0,2,4,6), plate velocity (U_{plate}=0.25,0.5,1,2) Reynolds number (Re=100,200,400), and nanoparticle vibration frequency (1Hz, 2Hz, 4 Hz ,8Hz) values were studied. While the plate velocity is changing, the nanoparticle volumetric concentration is taken as ϕ=4% and the Reynolds value is Re= 100. As a consequence, it was determined that while the plate is stationary, the impacting jet forms two symmetrical vortexes on the right and left sides of the plate. However, as the plate moves in the + x-direction, the thermal and velocity streamlines bend to the right. The stopping points of the jet flow were more apparent at low plate velocities. It was determined that the Nusselt number was maximum at these points, but this effect decreased with increasing plate velocities. It was determined that the total heat transfer rate increased as the nanoparticle volumetric concentration increased. It has been found that increasing the total heat transfer velocity with increasing the frequency for the vibratory jet impingement.

Buonomo et al. (2019) numerically investigated the flow and heat transfer analysis with the impinging jet technique of Al_2O_3-water nanofluid on a heated moving surface. Water and Al_2O_3-water nanofluid are used as working fluids. The k-ε turbulence model of ANYSYS FLUENT package program was used for the numerical model. Two geometric structure were created for two values of the jet target surface distance (H/W=6-10) in the research. The concentration of nanoparticles was researched in the range of ϕ=0%-6%, the Reynolds number was investigated at Re = 5000, 20000 values, and the plate velocity was investigated in the range of U_p=0,0.8,2 m/s. As a consequence, the moving plate decreased the local Nusselt number at the impact point substantially. The Reynolds value and plate velocity as increased, the average Nusselt number increased. The local Nusselt number increased, the volumetric ratio and jet--target surface distance ratio as increased. In the case of using nanofluid, in viscosity occurred an increase, so causing more entrainment of the moving plate. Thus, it has been determined that there is a greater mass flow rate from the moving surface.

Sharif and Banerjee (2008) numerically investigated the effect to heat transfer of a jet impinging to a heated moving plate. Jet outlet Reynolds number (Re=5000-20000), different plate velocities (U_{plate}=0-2 m/s) and jet- target plate distance (H/W=6-8) are the parameters examined in the study. The standard k-ε turbulence model was used for numerical analysis. As a result, when there is no movement in the plate and the jet hits the plate, two counter-rotating primary vortices were formed on either side of the jet. It has been determined that the increase in Jet Reynolds number and plate velocity provides a significant increase in the average Nusselt number.

Basaran and Selimefendigil (2013) studied numerically the heat transfer of jets double impinging to a moving plate heated for a laminar flow in a rectangular channel. Water and Al_2O_3-water nanofluid were used as working fluid. The effects of jet outlet Reynolds number (Re=50-200), plate velocity (U_p=0, 0.5, 1, 2 m / s) and nanofluid volumetric ratio (φ=0% - 6%) were investigated. FLUENT package program was used for numerical analysis. As a result, the Nusselt number increased as the plate velocity increased. The maximum increase in Nusselt number was obtained near the impact zone in the stationary plate at the exit in the moving plate. As the Re number increased, the thermal boundary layer became thinner and thus the heat transfer increased. It has been determined to increase the Nusselt number with increasing the nanoparticle volumetric ratio.

3. MATERIALS AND METHODS

In this study was numerically investigated the improvement of heat transfer from a moving surface with high heat flux by using the impinging fluid jet technique of nanofluids. The numerically is handled problem is solved regardless of time in cartesian coordinates. Elliptic equation type and shifted cell structure are used in the formulation of the equations. Mathematically steady viscous flows have an elliptical structure. This means that the values at one point of the flow are affected from the surrounding points. The hybrid scheme is used as the discretization process algorithm. This scheme is a scheme that combines the precision of the central differences scheme with the stability of the upwind scheme. It was used with the SIMPLEST (SIMPLEShorTened) algorithm, which is a variation of the SIMPLE algorithm as there is no direct equation for pressure.

The target plate dimensions are modeled as 110x40x32 cm (length x width x height). These dimensions were chosen for model the cooling using nanofluid and the impinging jet of a moving plate, which is high heat flux on the surface. The constant heat flux on the surface of the plate placed on the x-y plane is 222000 W/m^2. The nozzle hydraulic diameter is D_h=3.5 mm. For this numerical analysis, the low Re number k-ε turbulence model of PHOENICS HAD program was used. This model is preferred in confined impinging jet applications since it can obtain results compatible with the test results at the applied Reynolds value.

In the literature (Hremya et al. 1998) it is seen that the low Re number k-ε turbulence model gives the best results at Re=15000, but can be used up to Re=50000. For this reason, the operating range of Re value has been chosen as values close to this value in order to meet model criteria.

3.1. Model Geometry

Conservation of mass, momentum and energy equations are given in accordance with boundary conditions, the model is in continuous conditions. The heat transfer to the environment with radiation has been neglected, only the heat transfer with turbulent, forced convection is taken into account.

Conservation equations:

$$\frac{\partial U_i}{\partial x_i} = 0 \tag{3.1}$$

$$\rho U_i \ \frac{\partial U_j}{\partial x_i} = -\frac{\partial P}{\partial x_j} + \frac{\partial}{\partial x_i}\left[\mu\left(\frac{\partial U_i}{\partial x_j} + \frac{\partial U_j}{\partial x_i}\right) - \rho\overline{u_i^{'}u_j^{'}}\right] \tag{3.2}$$

$$\rho c_p U_i \ \frac{\partial T}{\partial x_i} = \frac{\partial}{\partial x_i}\left[k\frac{\partial T}{\partial x_i} - \rho c_p \overline{u_i^{'}T^{'}}\right] \tag{3.3}$$

Transport equations of the model:

$$\rho U_i \frac{\partial k}{\partial x_i} = \frac{\partial}{\partial x_i}\left[\left(\mu + \frac{\mu_t}{\sigma_k}\right)\frac{\partial k}{\partial x_i}\right] + \mu_t\left(\frac{\partial U_i}{\partial x_j} + \frac{\partial U_j}{\partial x_i}\right)\frac{\partial U_i}{\partial xj} - \rho\varepsilon \tag{3.4}$$

$$\rho U_i \frac{\partial \varepsilon}{\partial x_i} = \frac{\partial}{\partial x_i}\left[\left(\mu + \frac{\mu_t}{\sigma_\varepsilon}\right)\frac{\partial \varepsilon}{\partial x_i}\right] + f_1 C_1 \mu_t \frac{\varepsilon}{k}\left(\frac{\partial U_i}{\partial x_j} + \frac{\partial U_j}{\partial x_i}\right)\frac{\partial U_i}{\partial x_j} - f_2 C_2 \rho\frac{\varepsilon^2}{k} \tag{3.5}$$

Turbulent kinetic viscosity:

$$\mu_t = f_\mu C_\mu \rho\frac{k^2}{\varepsilon} \tag{3.6}$$

$\sigma_k = 1.00$; $\sigma_\varepsilon = 1.314$; $C_1 = 1.44$; $C_2 = 1.92$; $C_\mu = 0.09$

The damping functions of the Lam-Bramhorst low Reynolds number k-ε model are presented in the equations below.

$$f_\mu = \left[1 - exp(-0.0165 Re_z)\right]^2\left(1 + \frac{20.5}{Re_t}\right) \tag{3.7}$$

$$f_1 = \left(1 + \frac{0.05}{f_\mu}\right)^3 \tag{3.8}$$

$$f_2 = 1 - exp(-\mathrm{Re}_t^2) \tag{3.9}$$

In here,

$$Re_t = \frac{\rho k^2}{\mu \varepsilon} \tag{3.10}$$

$$Re_z = \frac{\rho k^{1/2} z}{\mu} \tag{3.11}$$

Jet inlet temperature is modelled as T_j=20°C. Model geometry is shown in Figure 3.1 and mesh structure is in Figure 3.2.

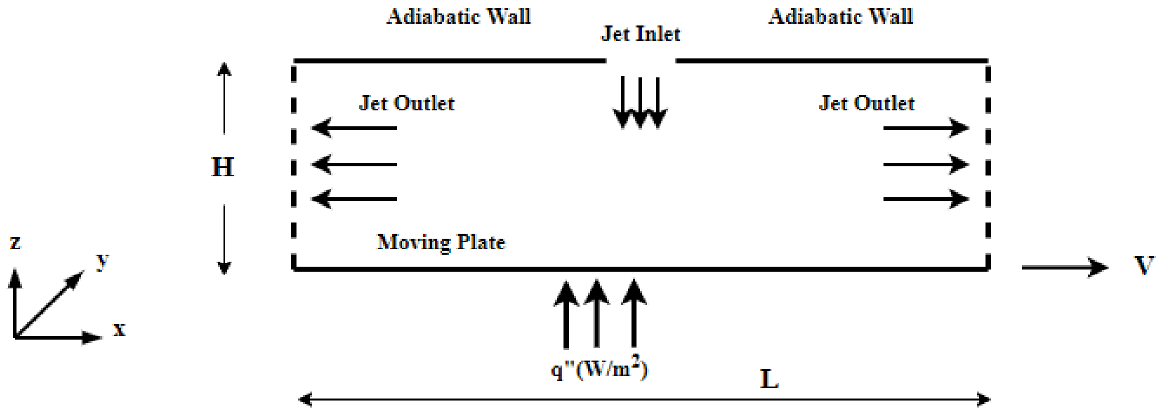

Figure. 3.1. CFD Model Geometry.

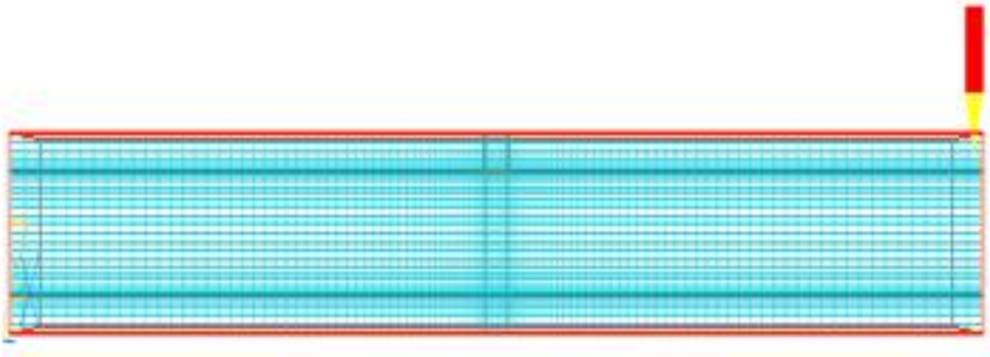

Figure. 3.2. Mesh Structure.

Boundary conditions in this study are shown below (Table 3.1)

Table 3.1. Boundary Conditions.

	U(m/s)	**V(m/s)**	**W(m/s)**	**T (K)**	**k**	**ε**
Jet	U=0	V=0	W= W_{inlet}	T=T_{inlet}	$(T_{\mathrm{i}} W_{jet})^2$	$(C_\mu C_d)^{3/4} \frac{k^{3/2}}{L}$
Plate	U=U_{plate}	V=0	W=0	q"=q"$_{surface}$	k=0	$\frac{\partial \varepsilon}{\partial z} = 0$
Outlet	$\frac{\partial U}{\partial x} = 0$	$\frac{\partial V}{\partial x} = 0$	$\frac{\partial W}{\partial x} = 0$	T=T_{outlet}	$\frac{\partial k}{\partial x} = 0$	$\frac{\partial \varepsilon}{\partial x} = 0$
Front Wall	U=0	V=0	W=0	$\frac{\partial T}{\partial y} = 0$	-	-
Upper Wall	U=0	V=0	W=0	$\frac{\partial U}{\partial z} = 0$	-	-

In this study, a mesh number of 110x40x32 (140.800) was used. The cell structure is adjusted according to the flow conditions, and the cells are concentrated on the surface of the jet inlet and the copper plate in order to obtain a more sensitive result. The iteration number was examined between 1000 and 5000 and the cell number was studied between 25 and 34. Accordingly, when the number of cells is 110x40x32 and the number of iterations is 3000, it has been observed that the results are independent of the number of cells and iterations.

Numerical model, Li Q. et al. (2012) has been verified according to the results of their experiment. As seen in Figure 3.3, the difference between the numerical model and experimental results is below 5% for Re=12000. In the current study, Re=16000 has been studied.

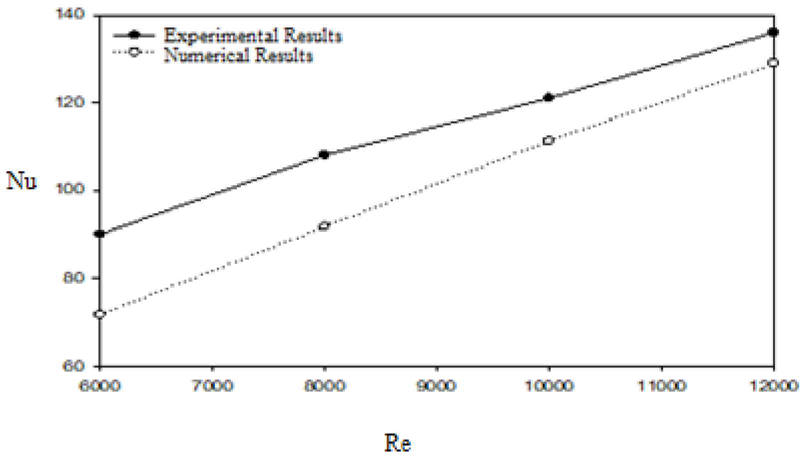

Figure. 3.3. Comparison of the numerical model.

3.2. Mathematical Formulation

Heat transfer from the plate surface will occur with, convection, conduction and radiation. Conduction and convection heat losses are neglected in the calculations.

$$Q_{convection} = Q_{total} - Q_{\mathrm{conduction}} - Q_{\mathrm{radiation}} \tag{3.12}$$

Heat transfer from the surface with convection;

$$Q_{convection} = h.A.\Delta T \tag{3.13}$$

As shown here, h is the heat transfer coefficient, A *is* convection surface area, ΔT ($\Delta T = T_{surface} - T_{bulk}$) is the difference between the measured surface temperature and the fluid average temperature.

Nusselt number (Nu) is a dimensionless parameter showing the ratio of convective heat transfer to conduction heat transfer. Therefore, the Nusselt number indicates the improvement in heat transfer in the fluid layers. The local Nusselt number indicates the improvement in locally occurring heat transfer, while the average Nusselt number indicates the improvement in heat transfer over the whole plate surface. Nusselt number;

$$Nu = \frac{(Q_{convection} D_h)}{(T_s - T_{jet}).k_{nf}} \tag{3.14}$$

As shown here, D_h is the hydraulic diameter, T_s is the measured surface temperature, T_{jet} is the jet inlet temperature, and, k_{nf} is the nanofluid thermal conductivity coefficient.

The Reynolds number (*Re*) is used to determine whether the flow is laminar or turbulent in forced convection. Reynolds number based on turbulent flow;

$$Re = \frac{(\rho_{nf}.V_{jet}.D_h)}{(\mu_{nf})} \tag{3.15}$$

As shown here, ρ_{nf} is the nanofluid density, V_{jet} is the jet outlet velocity, D_h is the hydraulic diameter, and μ_{nf} is the nanofluid dynamic viscosity. Density of the nanofluid is (Pak ve Cho, 1998);

$$\rho_{nf} = (1-\varphi).\rho_{bf} + \varphi.\rho_p \tag{3.16}$$

As shown here, φ is the nanofluid volume ratio, ρ_{bf} is the basic fluid (water) density, and ρ_p is the density of the solid particles in the nanofluid. Volumetric ratio of the nanofluid is;

$$\varphi = \frac{1}{(1/\omega).(\rho_p - \rho_{bf})} \tag{3.17}$$

As shown here, ω is the difference between the densities of the nanofluid and the basic fluid (water). Specific heat of nanofluid is (Wang et al., 2006);

$$C_{p_{nf}} = \frac{\varphi.(\rho.C_p)_p + (1-\varphi).(\rho.C_p)_f}{(\rho_{nf})} \tag{3.18}$$

As seen here, φ is the nanofluid volume ratio, $C_{p(p)}$ is the specific heat of the particle, $C_{p(f)}$ is the specific heat of the base fluid. The thermal conduction coefficient of the nanofluid is (Corcione, 2011);

$$\frac{k_{eff}}{k_f} = 1 + 4.4\,\mathrm{Re}_{(p)}^{\ 0.4}\,\mathrm{Pr}^{0.66}\left(\frac{T}{T_{fr}}\right)^{10}\left(\frac{k_p}{k_f}\right)^{0.03}\varphi^{0.66} \tag{3.19}$$

As seen here $Re_{(p)}$ is the nanoparticle Reynolds number, Pr is the Prandtl number of the base fluid. T is the temperature of the nanofluid (K), and T_{fr} is the freezing point of the base fluid. k_p is the thermal conduction coefficient of nanoparticles, φ is the particle volume ratio.
Nanoparticle Reynolds number is;

$$Re_p = \frac{2\rho_f k_b T}{\pi \mu_{bf}^2 d_p} \tag{3.20}$$

k_b is Boltzmann constant.
Dynamic viscosity of nanofluid is formulated as follows (Batchelor 1977);

$$\mu_{nf} = \mu_{bf}(1 + 2.5\varphi + 4.698\varphi^2) \tag{3.21}$$

As shown here, μ_{bf} is the dynamic viscosity of the base fluid, φ is the nanofluid volumetric ratio.

3.3. Verification of Numerical Results

In this thesis, the cell structure is adjusted according to the flow conditions, and the cells are concentrated on the jet inlets and the surface of the copper plate in order to obtain a more sensitive result. The iteration number was studied between 1000 and 5000; the cell number was studied between 25 and 34 (in the z-direction).

According to this, when the number of cells is 110x40x32 and the number of iterations is 3000, it has been seen that the results are independent from the number of cells and the number of iterations. In Figure 3.4 and Figure 3.5, the independent graphs from the cell number and iteration number are given.

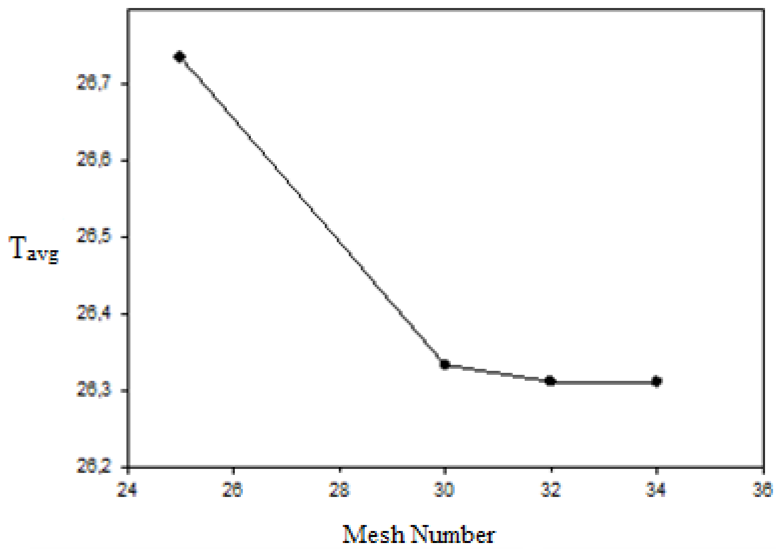

Figure. 3.4. Independence from the mesh number.

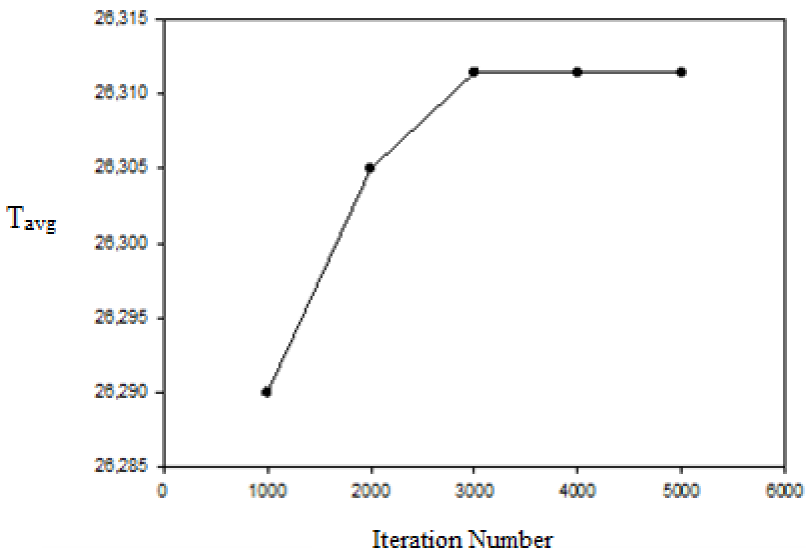

Figure. 3.5. Independence from the iteration number.

Reynolds values are between 12000-18000 in the current study. The low Reynolds number k-ε model, which is the turbulence model we use in turbulent flow modelling, needs a different cell structure than the standard k-ε model since it does not use wall functions. In the light of this information, the density of the cells was increased in order to capture the changes in the boundary layer and to model the viscous substrate boundary in the areas close to the impact plate in the solution area.

It has been determined that the difference between the numerical results and the experimental results obtained in the case of using the low Re number k-ε turbulence model is less than 5% for Re=12000. The low Re number k-ε turbulence model was compared with the standard k-ε turbulence model and the standard k-ω turbulence model, and it was found that it could better represent the experimental results. Comparison of numerical results obtained by using different turbulence models for Cu-H_2O nanofluid with experimental results is shown in Figure 3.6.

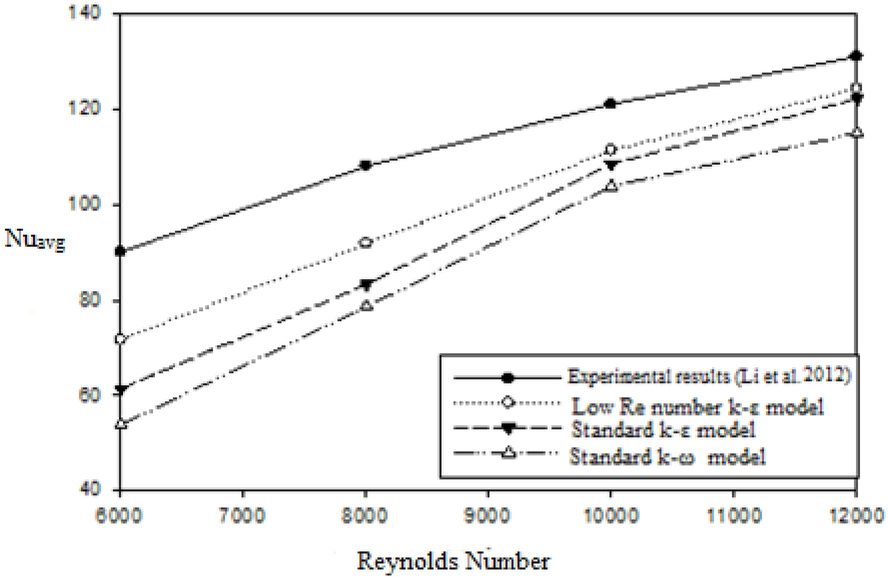

Figure. 3.6. Comparison of model results with experimental results (φ = 1.5%) for Cu-H_2O nanofluid (Li et.al., 2012).

4. RESULTS AND DISCUSSION

In this section, the numerical results were taken for 6 different parameters. The thesis study was examined in two stages. In the first stage, the Cu-H_2O nanofluid was studied for a stationary plate and the model was verified, in the following study, the heat transfer and flow properties in both a moving and stationary plate of the Al_2O_3-H_2O nanofluid were examined.

a) Stationary Plate

- Effect to heat transfer at different Reynolds numbers of Cu-H_2O nanofluid (Re= 12000, 14000, 16000, 18000; V_{plate}=0 m/s)
- Effect to heat transfer at different particle diameters of Cu-H_2O nanofluid (D_p=10nm, 20nm, 40nm, 80nm; V_{plate}=0 m/s)

b) Moving / Stationary Plate

- Effect to heat transfer at different particle diameters of Al_2O_3-H_2O nanofluid (D_p=10 nm, 20nm, 30nm, 40nm; V_{plate}=2 m/s)
- Effect to heat transfer at different plate velocities of Al_2O_3-H_2O nanofluid (V_{plate}=0 m/s, 2 m/s, 4 m/s, 6 m/s)
- Effect to heat transfer at different volume ratios of Al_2O_3-H_2O nanofluid (φ =0.5%, φ =1%, φ =1.5%, φ =2%; V_{plate}=2 m/s)
- Effect to heat transfer of different types of nanofluids (Cu-H_2O, Al_2O_3-H_2O, TiO_2-pure water; V_{plate}=2 m/s) was investigated.

4.1. Effect to Heat Transfer at Different Reynolds Numbers of Cu-H_2O Nanofluid

In this parameter, the effect on heat transfer of different Reynolds numbers was researched for an impinging jet created using Cu-H_2O nanofluid (20 nm particle diameter, 4% volumetric ratio) (Re=12000, 14000, 16000, 18000). The effect to the local Nusselt number of jets on different Reynolds numbers is shown in Figure 4.1.

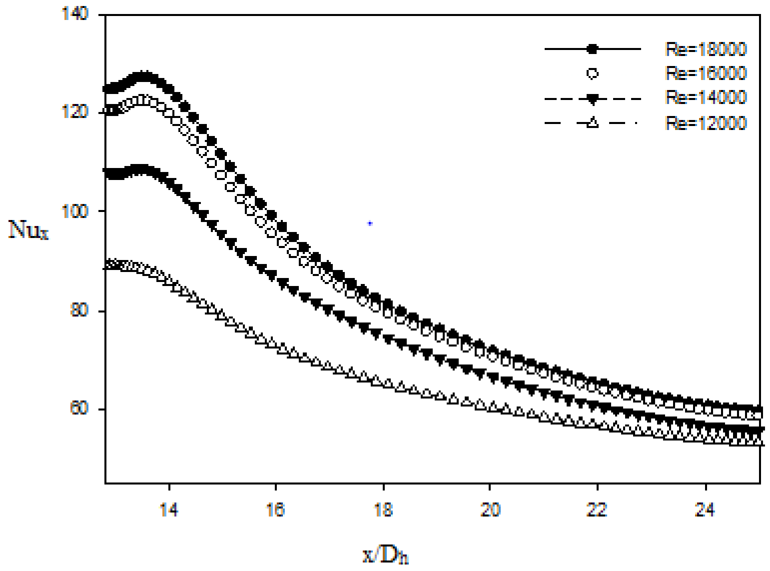

Figure. 4.1. Change of local Nusselt number at different Reynolds numbers (dp=20 nm and φ= 4%) of the Cu-H_2O nanofluid.

Reynolds (Re) number was increased from Re=12000 to Re=18000, and the average Nusselt Number (Nu_{avg}) also increased, but it was determined that this increase continued to decrease. In the impact zone, the local Nusselt number decreased somewhat due to the decrease in velocity as expected. The local Nusselt number due to the velocity to depend on the momentum transfer at the beginning of the wall jet zone has been highest level. Local Nusselt number decreased due to surface friction in the wall jet area. The change in local Nusselt number for different Reynolds numbers was similar. However, the difference in the local Nusselt number is the highest in the impact, this difference gradually is determined decreases in the wall jet zone.

Increase in average Nusselt number is 14% value in the range Re=12000-14000; it is 8.9% between Re=14000-16000 and it is 2.9% between Re=16000-18000. Thus; as a result of increasing the value from Re=12000 to Re=18000, it was determined that there was an increase of 28% in the average Nusselt number.

Current result, when compared with the studies in the literature (Lv et al. 2012; Wang et al. 2006), the increase in the number of Re and the increase in heat transfer is similar in the studies in the literature. In addition, it was determined that the change in the local Nusselt number in the impact zone and the wall jet region was similar to the studies in the_literature.

However, compared to the one phase models of two-phase models has been observed that it represents the physical process better. Temperature contours at Re=12000 and Re=18000 values are shown in Figure 4.2, and velocity vectors at Re=12000 and Re=18000 values are shown in Figure 4.3.

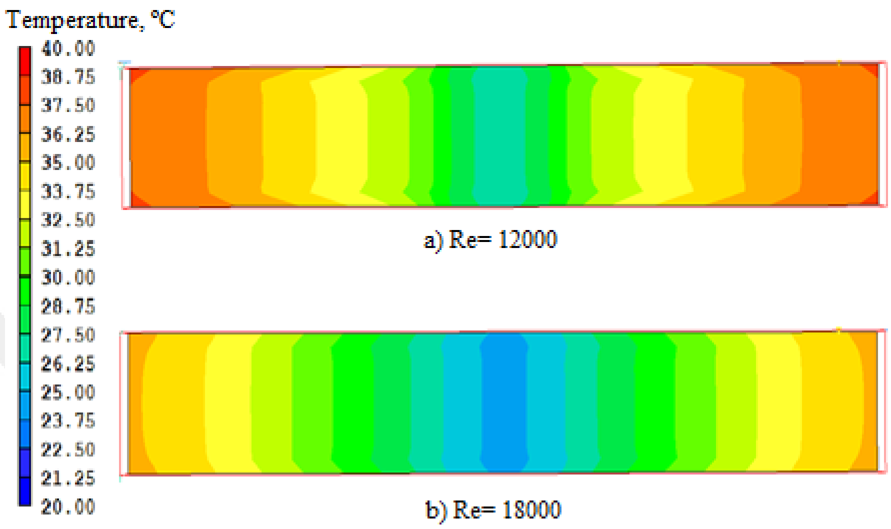

Figure. 4.2. Temperature contours of Cu-H_2O nanofluid for a) Re=12000 and b) Re=18000 (dp =20 nm and φ=4%).

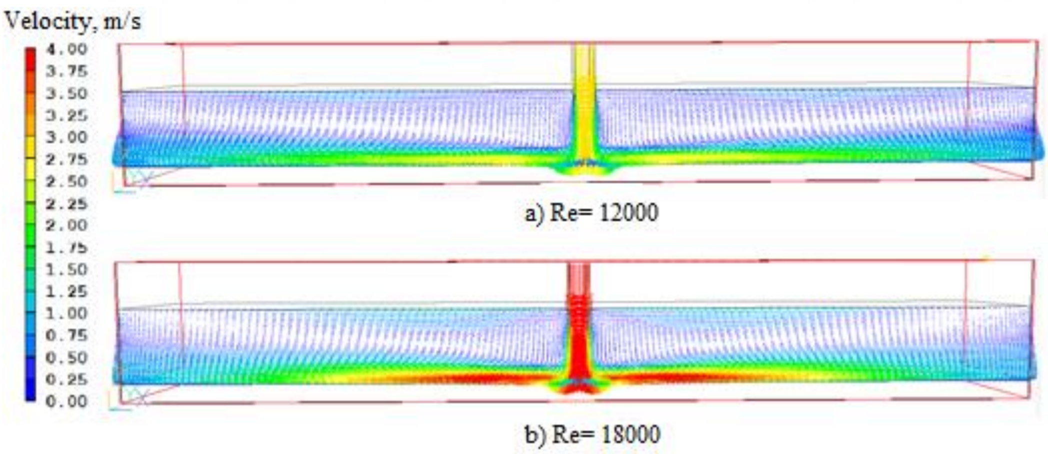

Figure. 4.3. Velocity vectors of Cu-H_2O nanofluid for a) Re=12000 and b) Re=18000 (dp=20 nm and φ= 4%).

The impact point is the most seen place of the jet effect. The fluid velocity has increased as the increase of Re number. Increasing fluid velocity enabled the secondary vortexes in this zone to remain in a more limited area. Therefore, the temperature decrease was higher at the impact point, but it occurred in a more limited area. The fluid that changes direction after impact accelerates due to momentum transfer. This situation has protected up to farther distance in the wall jet zone of velocity with the Re number increases. Thus, it has determined to provide up to farther distance the temperature decrease of the fluid accelerated with the momentum transfer. It has been seen that the thermal boundary layer thickness and surface temperatures increase due to the decrease in fluid velocity in the zones close to the channel walls. However, this effect decreases as the Re number increases. Since the impact plate is copper (material with a high coefficient of thermal conductivity), it has been observed that the local cooling effect provided on the impact plate rapidly spreads over the whole plate. This case provides to occur in regularly of the temperature changes on the plate surface.

The result indicated that, when Cu-H_2O nanofluid is used (20 nm particle diameter and 4% volumetric ratio), it has been determined to increase expectedly of the heat transfer with the increase in the Re number. As a result of increasing the Re number from 12000 to 18000, it was determined that there was an increase of 28% in the average Nusselt number.

4.2. Effect to Heat Transfer at Different Particle Diameters of Cu-H_2O Nanofluid

In this parameter, the copper nanoparticles in the basic fluid in different diameters (D_p=10nm, 20nm, 40nm, 80nm) are studied for 4% volumetric ratio, Re=16000. In Figure 4.4, local Nusselt numbers achieved for different nanoparticle diameters are shown.

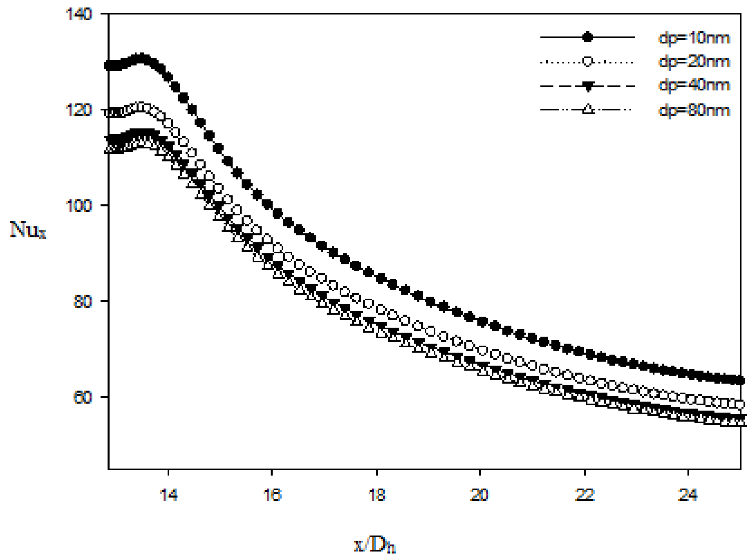

Figure. 4.4. Effect to local Nusselt number of different particle diameters.

As the nanoparticle diameter used in the fluid decreases, the surface area/volume ratio of the particles increases, which causes an increase in the surface area between the solid particle and the basic fluid, thus it causes an increase in heat transfer from the nanofluid. Also, in small diameter particles, the hydrodynamic behaviour resulting from the impact and translational motion (Brownian motion) also increases the formation of the vortex. This case increases the hydrodynamic boundary layer and it decreases the thermal boundary layer.

According to these results, when the particle diameter was 10nm, the best heat transfer performance was obtained. When the particle diameter was reduced from 80nm to 10nm, there was an increase by 13.2% in the average Nusselt number. The change in the local Nusselt number is show similarity across the target plate. The local Nusselt number is the highest level due to the high velocity at the beginning of the wall jet zone however, it is decreasing gradually due to the decrease in velocity in the wall jet zone. The difference in local Nusselt number is highest at the beginning of the wall jet zone in the range in particle diameter.

The reason for this is that in small particle diameter nanofluids has a larger heat transfer surface area. Furthermore, it has a higher turbulent density due to high velocity. The reduction in the local Nusselt number is minimum throughout the wall jet zone at D_p=10 nm. This is because; since the particle diameter is small, it is affected to less from the friction effects between the fluid layers. Temperature contours for D_p=10 nm and D_p=80 nm are shown in Figure 4.5, velocity vectors for D_p=10 nm and D_p=80 nm are shown in Figure 4.6.

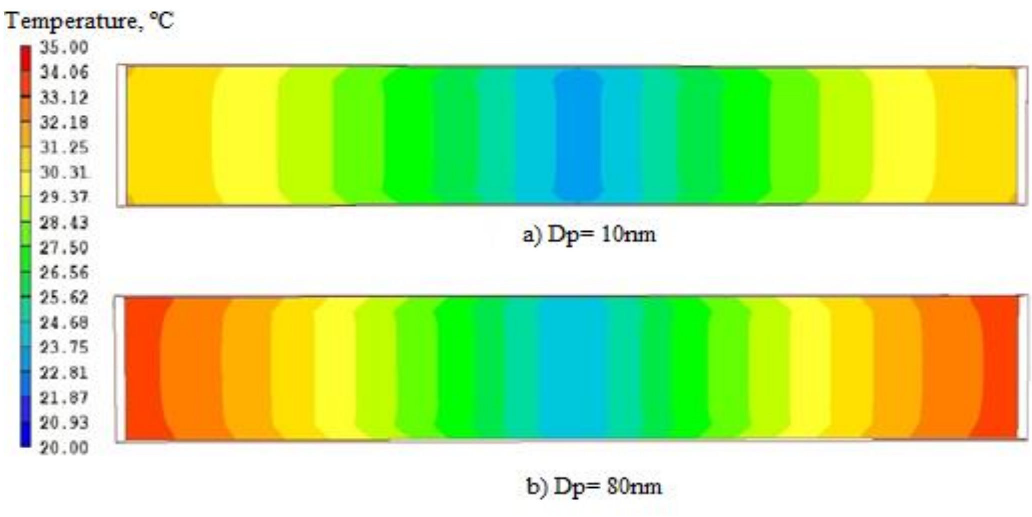

Figure. 4.5. Temperature contours of the Cu- H_2O nanofluid for a) D_p=10 nm and b) D_p= 80 nm (Re = 16000 and φ = 4%).

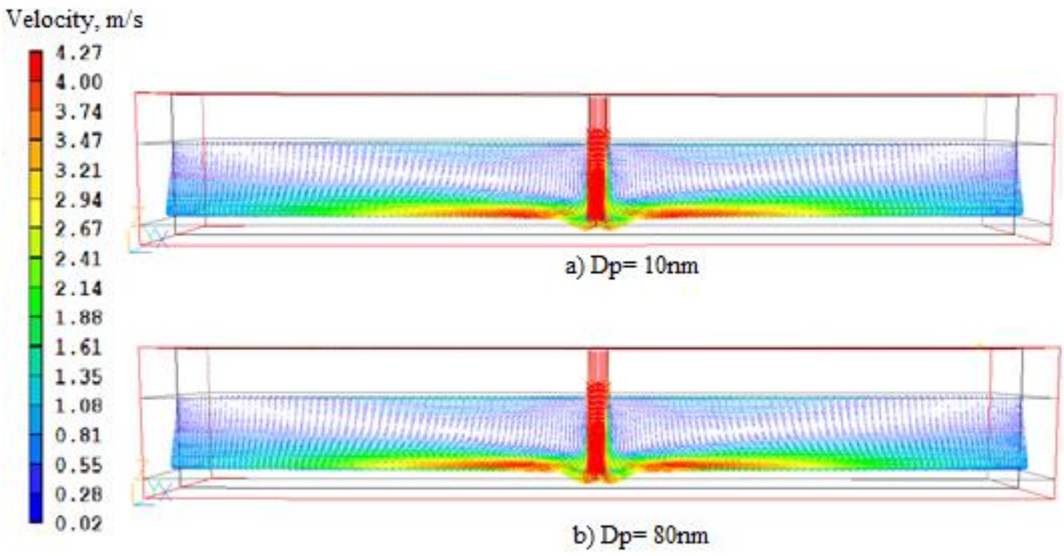

Figure. 4.6. Velocity vectors of the Cu- H_2O nanofluid for a)D_p=10 nm and b)D_p=80 nm (Re=16000 and φ=4%).

As the particle diameter decreases; a gradually increasing increase in the average Nusselt number (Nu_{avg}) was determined. When the particle diameter is reduced from 80 nm to 40 nm, Nu_{avg} was increased by 2%; when the particle diameter was reduced from 40nm to 20nm, Nu_{avg} was increased by 6%, and when the particle diameter was reduced from 20nm to 10nm, Nu_{avg} was increased by 8%.

The reasons for this are the increase in the nanofluid heat transfer coefficient due to the reducing particle diameter and the vortexes are created in the regions close to the surface. These vortexes are occurred by the collision and translational motion (Brownian motions) of the nanoparticles.

Current result, when compared to the studies in the literature (Li et al. 2012; Feng and Kleinstreuer 2006), there are not many studies that primarily examine the particle diameter as a parameter in the literature. Similar to the current studies, an increase in heat transfer was found to depend on the decrease in nanoparticle diameter also in this study. In the literature, when reduction of 10 nm in particle diameter, Nusselt number is seen increase by 5.7% (φ= 4% volumetric ratio and D_p=20-40 nm). In this parameter had been obtained an increase of 6% under the same conditions.

The result shows that it has been determined that as the nanoparticle diameter used decreases in the fluid, the heat transfer increases occur increase in the heat transfer coefficient of the fluid, the heat transfer increase with increase the particle surface area/volume ratio. It has been found that when the particle diameter is reduced from 80nm to 10nm, in the average Nusselt number has been observed an increase of 13.2%.

4.3. Effect to Heat Transfer at Different Particle Diameters of Al_2O_3-H_2O Nanofluid

In this parameter, the effect to heat transfer of different particle diameters (D_p=10nm, 20nm, 30nm, 40nm) was investigated for an impinging jet created using Al_2O_3-H_2O nanofluid. Jet inlet temperature is T_{inlet}=20ºC, Re=16000 and plate velocity is V_{plate}=2 m/s. In Figure 4.7, local Nusselt numbers obtained for different nanoparticle diameters are shown. In Figure 4.8, the change of the average Nusselt number is given.

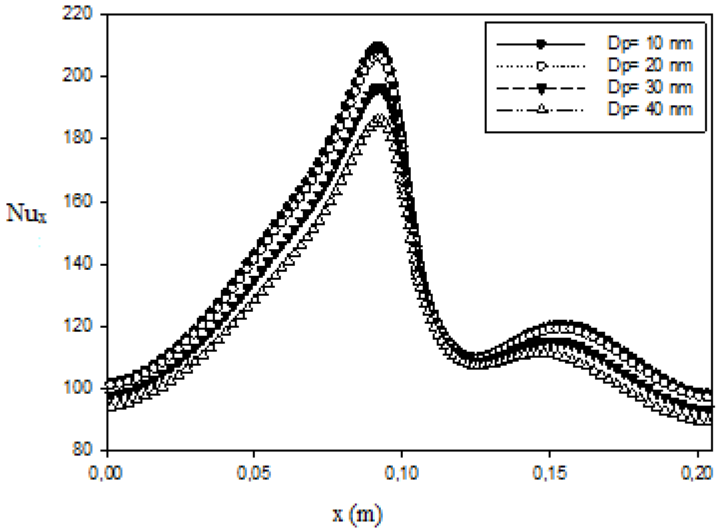

Figure. 4.7. Effect to local Nusselt number of different particle diameters.

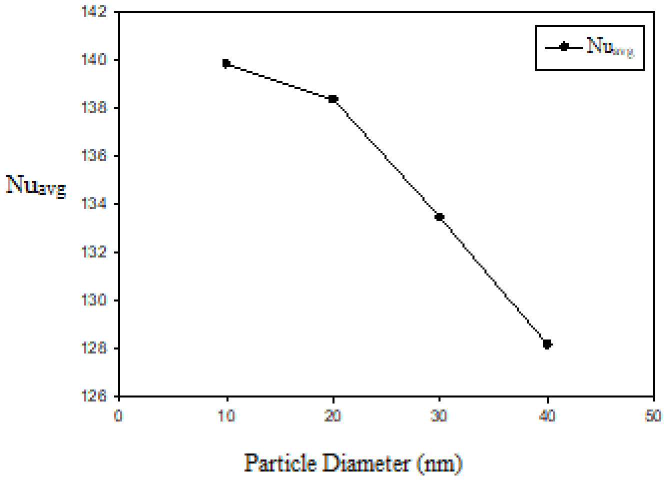

Figure. 4.8. Effect to average Nusselt number of different particle diameters.

It has been determined that as the nanofluid particle diameter decreases (depending on the increase of solid particle surface area) the average Nusselt number increases and the surface temperature decreases. However, this increase in the average Nusselt number has been continued as decreasing for decreasing particle diameters. It has been determined that when the particle diameter is reduced in the range D_p=40-30 nm that there is a 4.1% increase in the average Nusselt number, when reduced in the D_p=30-20 nm range that there is a 3.7% increase in the average Nusselt number, when reduced in the D_p=20-10 nm range that there is a 1.1% increase in the average Nusselt number.When it was decreased in the range of D_p=40-10nm, the highest heat transfer increase occurred as an increase of 9.1% in the average Nusselt number. Temperature contours occurred on the plate surface are shown for D_p=10nm and D_p=40nm values in Figure 4.9.

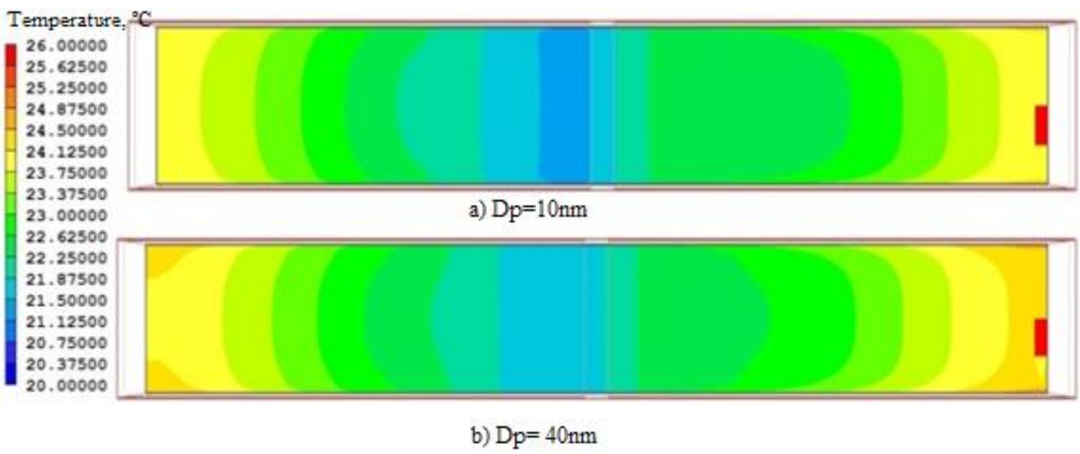

Figure. 4.9. Plate temperature contours of Al_2O_3-H_2O nanofluid for a) D_p=10 nm and b) D_p= 40 nm.

As a result, it has been determined that as the nanofluid particle diameter reduces (depending on the increase of solid particle surface area) the average Nusselt number rise and the surface temperature reduces. However, this increase in the average Nusselt number has been continued as decreasing for decreasing particle diameters. When reduced in the D_p=40-10nm range that there is a 9.1% increase in the average Nusselt number.

4.4. Effect to Heat Transfer at Different Plate Velocities of Al_2O_3-H_2O Nanofluid

In this parameter, the effect to heat transfer of different plate velocities (V_{plate}= 0 m/s, 2 m/s, 4 m/s, 6 m/s) was investigated for an impinging jet created using Al_2O_3-H_2O nanofluid. Nanofluids have a volumetric ratio of ϕ=2.0. The jet inlet temperature is T_{inlet} = 20ºC, and the Reynolds number is Re=16000. Change of the local Nusselt numbers obtained for different plate velocities are given in Figure 4.10, and the change of the average Nusselt number is given in Figure 4.11.

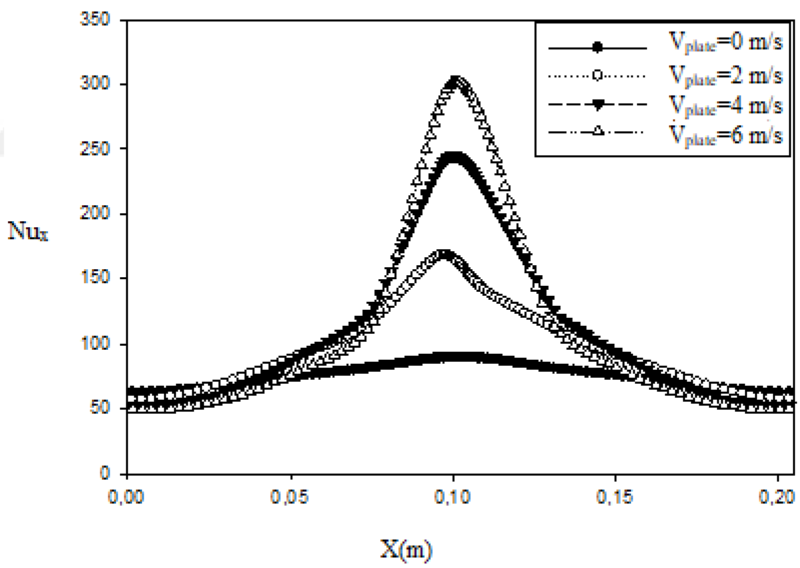

Figure. 4.10. Effect to local Nusselt number of different plate velocity.

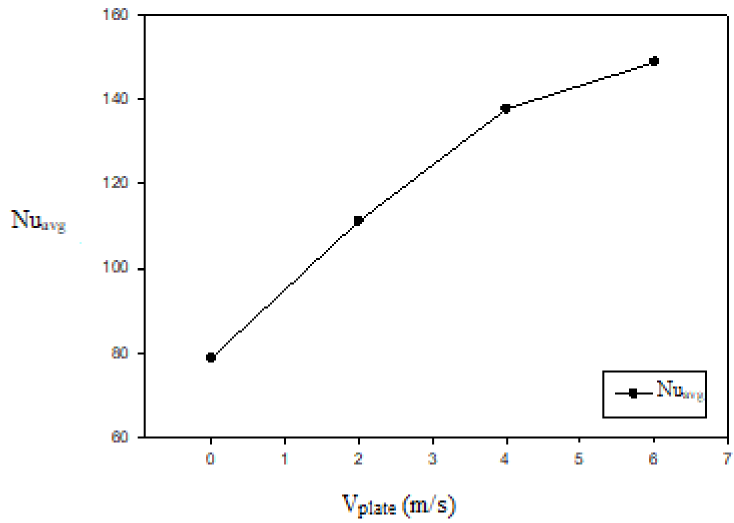

Figure. 4.11. Effect to average Nusselt number of different plate velocity.

It has been determined that as the plate velocity increases, the local Nusselt number increases, especially in the impact zone, the high heat transfer effect provided in the impact zone changes in the opposite direction of the plate movement direction. It was determined that depend on the increase of the plate velocity also the average numbers are increased, but this increase continues by decreasing. It has been determined that the local Nusselt numbers occurring at low velocities are lower for fluid flowing in the direction of plate movement, and in the opposite direction occurring of local Nuselt numbers are higher.

It can be said that the reason for this is that, the velocity of the flow is in the same direction depending on the plate movement and the hydrodynamic boundary layer decreases in the region where is in the opposite direction and due to the heat boundary layer increases.

As the plate velocity increases at different plate velocities, it has been determined that the average Nusselt number increases prominently. However, it has been determined that this increase continues by decreasing as the plate velocity increases. It has been determined that as the plate velocity increases, the hydrodynamic boundary layer increases, so the thermal boundary layer decreases and the heat convection coefficient increases. When plate velocity is increased in the range of V_{plate}=0-2 m/s, increasing in Average Nusselt number is 40.9%; when plate velocity is increased in the range of V_{plate}=2-4 m/s, increasing in average Nusselt number is 23.9%; and when plate velocity is increased in the range of V_{plate}=4-6 m/s, increasing in average Nusselt number is determined 8.1%. Figure 4.12 shows the temperature contours that occur on the impact plate for different plate velocities.

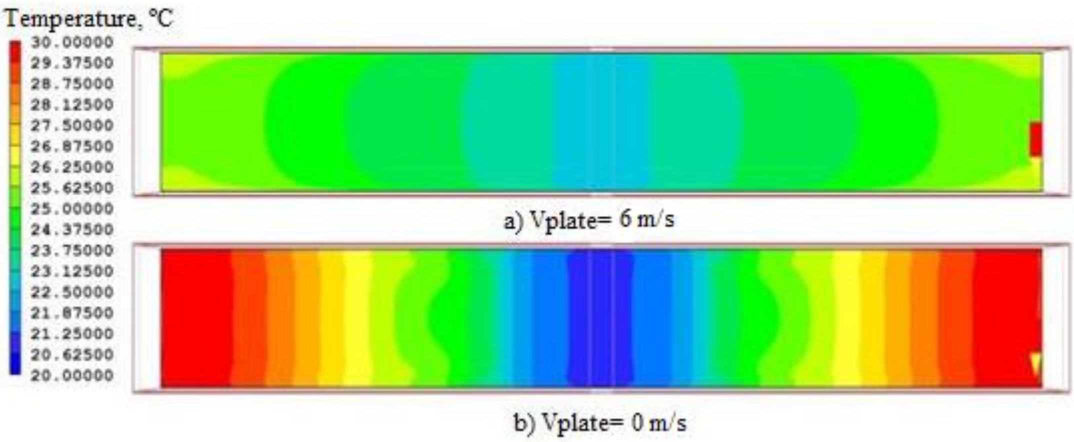

Figure. 4.12. Plate Temperature contours of Al_2O_3-H_2O nanofluid for a) V_{plate}=6 m/s and b) V_{plate} = 0 m/s.

To sum up, it was determined that as the plate velocity increased, the Average Nusselt number increased prominently. It has been observed that as the plate velocity increases, the hydrodynamic boundary layer increases and consequently the thermal boundary layer decreases and the coefficient of the heat convection increases. It has been determined that when plate velocity is the increased range of V_{plate}=0-6 m/s, the average Nusselt number is increased by 88.9%.

4.5. Effect to Heat Transfer at Different Volume Ratios of Al_2O_3-H_2O Nanofluid

In this parameter, the effect to heat transfer of different volumetric ratios (ϕ= 0.5%, 1%, 1.5%, 2%) was investigated for an impinging jet created using Al_2O_3-H_2O nanofluid. Jet inlet temperature is T_{inlet}=20ºC, Re=16000 and plate velocity is V_{plate}=2 m/s. The local Nusselt numbers are given for different volume ratios in Figure 4.13, and the change of the average Nusselt number is given in Figure 4.14.

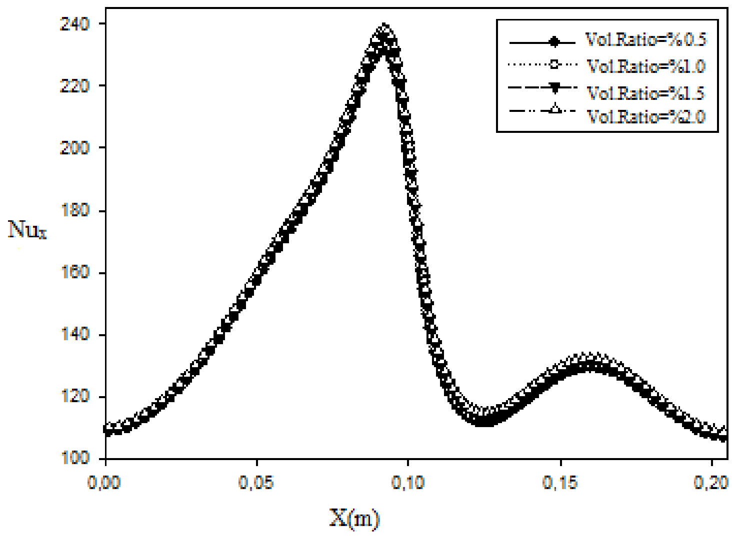

Figure. 4.13. Local Nusselt numbers at different volume ratios.

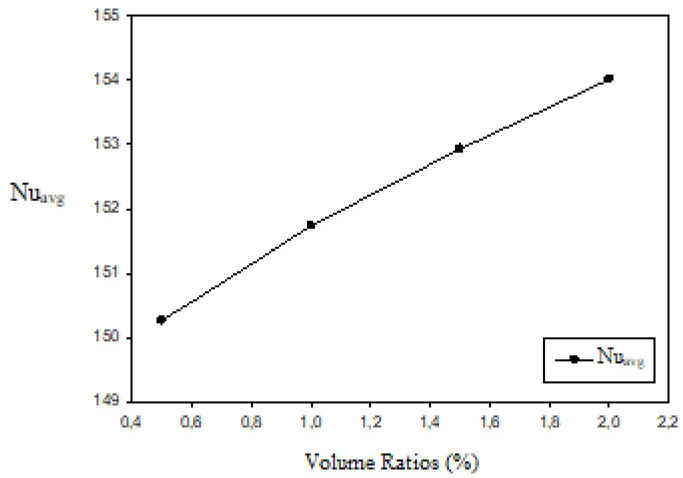

Figure. 4.14. Average Nusselt numbers at different volume ratios.

It has been determined that as the volumetric ratio is increased, the heat transfer from the plate is increased, but this increase continues by decreasing. When the volumetric ratio is increased in the range of ϕ=0.5-1.0, increasing in average Nusselt number is 0.98%; when the volumetric ratio is increased in the range of ϕ=1.0-1.5, increasing in Average Nusselt number is 0.79%; and when the volumetric ratio is increased in the range of ϕ=1.5-2.0, increasing in average Nusselt number is determined 0.71%. Temperature contours occurred on the plate surface are shown for volumetric ratios ϕ = 0.5 and ϕ = 2.0 in Figure 4.15.

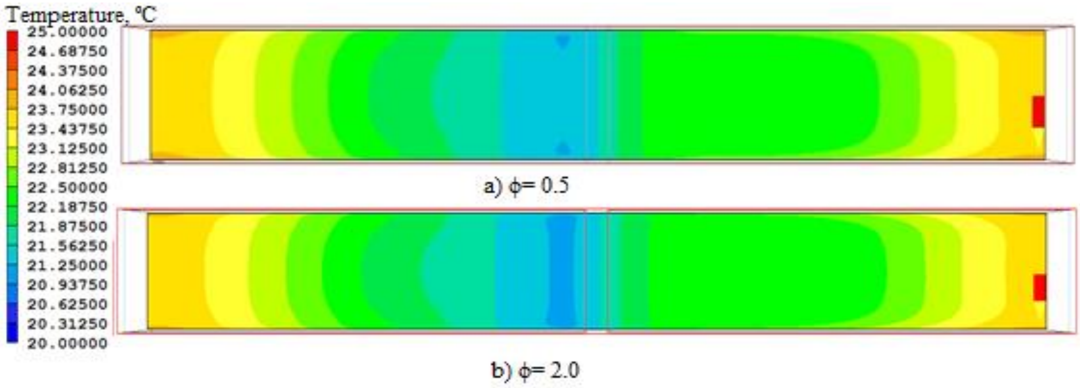

Figure. 4.15. Plate temperature contours of Al_2O_3-H_2O nanofluid for a) ϕ=0.5 and b) ϕ=2.0.

As a result; it was determined that as the volumetric ratio of nanofluid increased (due to the increase of the number of particles in the fluid), the average Nusselt Number increased and the surface temperature decreased. However, it has been determined that this increase in the average Nusselt number continues by decreasing for increasing volumetric ratios. When the volumetric ratio is increased in the range of ϕ=0.5-2.0, it has been determined increase by 2.5% in the average Nusselt number.

4.6. Effect to Heat Transfer of Different Types of Nanofluids

In this parameter, using different types of nanofluids (Cu-H_2O, Al_2O_3-H_2O, TiO_2-water and pure water) the effect to heat transfer an impinging jet was investigated. Nanofluids have a volumetric ratio of ϕ=2.0. Jet inlet temperature is T_{inlet} =20ºC, Re=16000 and plate velocity is V_{plate}=2 m/s. Table 4.1 gives thermophysical properties of nanofluids at 20 ºC.

Table 4.1. Thermophysical properties of nanofluids at 20ºC.

Nanofluid	**Density ρ(kg/m^3)**	**Specific Heat Cp(J/kgK)**	**Dynamic Viscosity, µ(Pa.s)**	**Kinematic Viscosity (m^2/s)**	**Thermal Conductivity Coefficient λ (W/mK)**	**Thermal Expansion Coefficient β (m^2/s)**
Cu-H_2O	1316.672	3148.451	0.001099	0.000000835	0.6684	0.000161
Al_2O_3-H_2O	1055.836	3931.451	0.001044	0.000000989	0.6391	0.000154
TiO_2-H_2O	1063.236	3902.513	0.001044	0.000000982	0.6378	0.000153
Pure water	998.2	4182.0	0.000993	0.00000099	0.597	0.000143

Local Nusselt numbers are given for different types of nanofluids in Figure 4.16, and the change of average Nusselt numbers of different types of nanofluids are given in Figure 4.17.

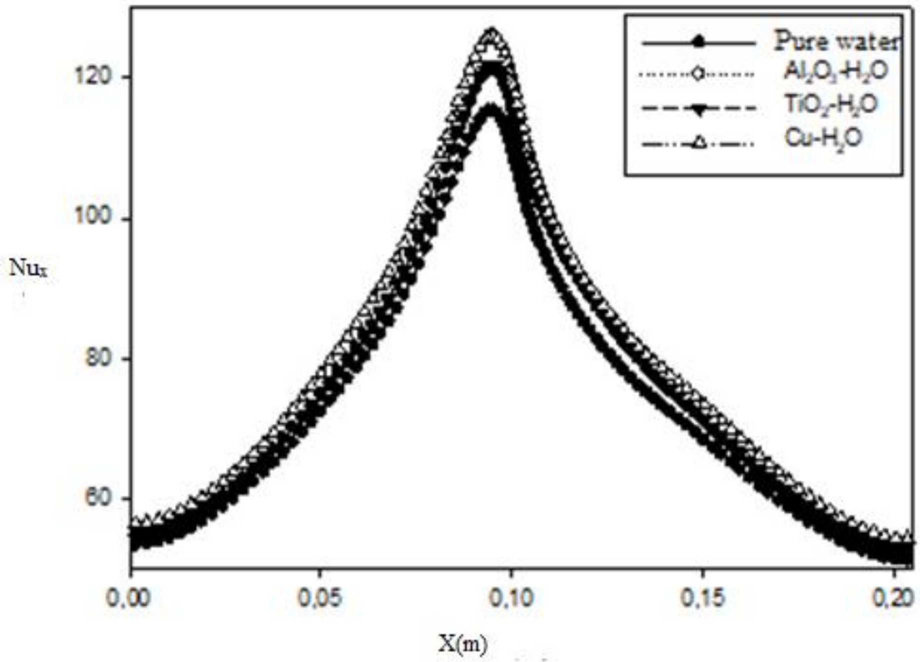

Figure. 4.16. The effect on the local Nusselt number of different nanofluids.

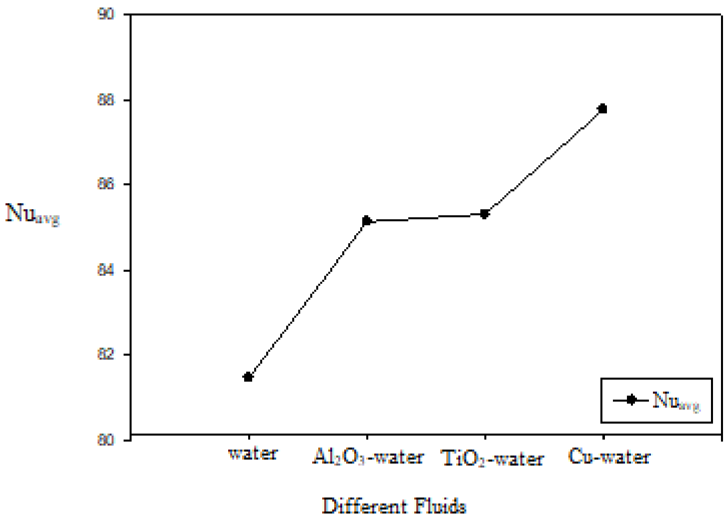

Figure. 4.17. The effect on the average Nusselt number of different nanofluids.

It has been determined that nanofluids show similar flow properties in the same volumetric ratio and Reynolds number.

It was determined that Cu-H_2O nanofluid showed the best heat transfer performance. In the case of using Cu-H_2O nanofluid; it was determined that the average Nusselt number increased 2.9% compared to TiO_2-H_2O, 3.1% compared to Al_2O_3-H_2O nanofluid, and 7.7% compared to pure water. It has shown in nanofluid, which is the highest heat conduction coefficient of the highest increase in heat transfer. Therefore, it has been determined the nanofluid heat conduction coefficient is an important parameter. Also, it has been determined that the use of nanofluid can provide a significant increase in heat transfer compared to conventional heat transfer fluids (water). The temperature contours occurring is shown on the impact plate for different nanofluids in Figure 4.18.

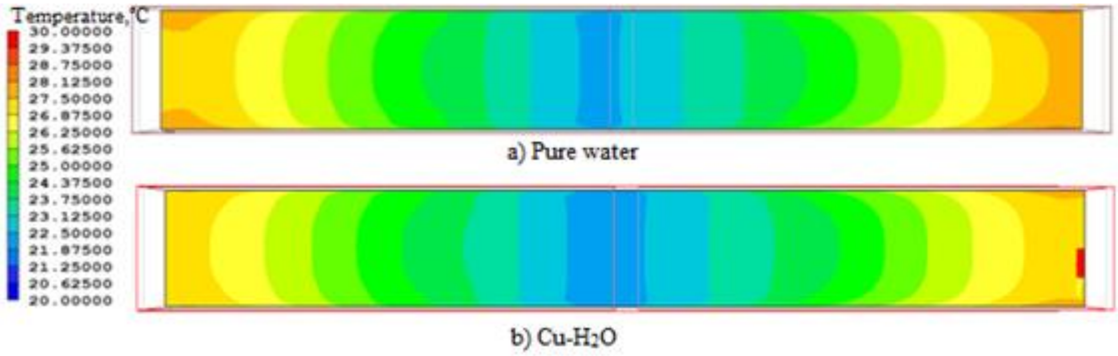

Figure. 4.18. Plate Temperature contours a) Pure water, b) Cu-H_2O.

As a result, it was determined that Cu-H_2O nanofluid showed the best heat transfer performance in the case of using different nanofluids.

5. CONCLUSIONS

The aim of this thesis study is to examine the heat transfer and flow properties in cooling with different types of nanofluid, which is heat transfer from a moving plate with high heat flux using a single air jet. In the current studies in the literature, there are some separately studies on the determination of the material characteristics of nanofluids and the effect on heat transfer of impinging jets. Unlike the studies in the current literature, the common effect of impinging jet and nanofluid were numerically investigated effect at the heat transfer from a moving plate with the using impinging jet technique.

In order to the cooling of systems with high heat flux;

- The different Reynolds numbers of the Cu-H_2O nanofluid
- Different particle diameters of Cu-H_2O nanofluid
- Different particle diameters of Al_2O_3-H_2O nanofluid
- Plate velocities of Al_2O_3-H_2O nanofluid
- Volume ratios of Al_2O_3-H_2O nanofluid
- The effect of different types of nanofluids on heat transfer has been investigated.

In the thesis study, the low Re number k-ε turbulence model of the PHOENICS computational fluid dynamics program was used.

In the numerical study, the problem has been defined, the model geometry has been created, and the necessary calculations have been made on the boundary conditions. The model has been independent from the number of cells and the number of iterations, after the pre-model results are seen compatible with the existing studies in the literature, the model study has been completed in accordance with the model program. Numerical study has been verified and interpreted with existing studies in the literatüre.

The iteration number was studied between 1000-5000 and the cell number was studied in the range of 25-34. When the number of cells is 110x40x32 and the number of iterations is 3000, it has been determined that the results are independent from the number of cells and iterations. The numerical model has been validated by experimental studies available in the literature.

According to the result of the study,

- In the case of using Cu-H_2O nanofluid (stationary plate), it has been determined that heat transfer increases with increasing Reynolds number, and it was determined an increase by 28% in the average Nusselt number with increasing from Re=12000 to Re=18000.
- In the case of using Cu-H_2O nanofluid (stationary plate), it was found that heat transfer increases as the nanoparticle diameter decreases and when the particle diameter was reduced from D_p=80 nm to D_p=10 nm, in the average Nusselt number was determined increase by 13.2%.
- In the case of using Al_2O_3-H_2O nanofluid, it has been determined that as the nanoparticle diameter decreases, the average Nusselt number increases and the surface temperature decreases, when the particle diameter was reduced from D_p=40 nm to D_p=10 nm, in the average Nusselt number was determined increase by 9.1%.
- In the case of using Al_2O_3-H_2O nanofluid, it has been determined that as the plate velocity increases, the average Nusselt number increases, and when the plate velocity was increased from V_{plate}=0 m/s to V_{plate}=6 m/s, in the average Number was determined increase by 88.9%.
- In the case of using Al_2O_3-H_2O nanofluid, it was determined that as the volumetric ratio increases, the average Nusselt number increases and the surface temperature decreases, and when the volumetric ratio is increased from φ=0.5 to φ= 2.0, in the average Number was determined increase by 2.5%.
- In the case of using different nanofluids (Cu-H_2O, Al_2O_3-H_2O, TiO_2- pure water), it was determined that Cu-H_2O nanofluid showed the best heat transfer performance. It has been determined that Cu-H_2O nanofluid provides 7.7% better heat transfer compared to pure water.

6. RECOMMENDATIONS

The results of this thesis study, it can be used in industry, and it can use in aviation and space technology in the design of more efficient heat exchangers. Then, it can use in systems, which is high cooling needs such as the cooling of electronic systems, solar collectors, and nuclear technology. In addition, it will be able to contribute to the development of health, robotic applications, automotive, defence, aviation and space technologies in the future.

In the future studies related to this thesis topic;

- It can be studied on heat transfer effects and to flow properties of the common effect of hybrid nanofluids and ferromagnetic nanofluids together with impinging jets.
- New studies can be conducted to examine the effects of single and multiple jets on different jet geometries using nanofluid.
- New studies can be made on the use with different surface cooling techniques (film cooling, cooling by perspiration, etc.) of impinging jets in case of using nanofluidic fluid.
- Most of the researches in the literature has been carried only for spherical nanoparticles. In future studies, the production of nanoparticles of different geometries (such as hexagon, triangle, square, oval) produced in different diameters, determination of the thermal properties of these new types of nanofluids which are produced, about the effect to flow characteristics and heat transfer of these fluids can be investigated.
- Energy management based studies can be done about economic analysis of new types of nanofluids and their effect on the environment.
- Studies can make to the effect flow characteristic and on heat transfer of different types nanofluids using impact plates, which are different surface roughness values such as metal foams.

REFERENCES

Abdelrehim, O., Khater, A., Mohamad, A. A., Radwan, A. (2019). Two-phase simulation of nanofluid in a confined single jet. Case Studies in Thermal Engineering, 14, 100423.

Asadi, A., Aberoumand, S., Moradikazerouni, A., Pourfattah, F., Żyła, G., Estellé, P.,Arabkoohsar, A. (2019). Recent advances in preparation methods and thermophysical properties of oil-based nanofluids: A state-of-the-art review. Powder Technology, 352, 209-226.

Assef, Y., Arab, D., Pourafshary, P.,(2014). "Application of nanofluid to control the fines migration to improve the performance of low salinity water flooding and alkaline flooding ", J. Pet. Sci. Eng., vol.124, pp.331-340.

Aytaç, İ. (2020). Hibrit Nanoakışkanların Termofiziksel Özelliklerinin Isıl Davranışları. Gazi Üniversitesi Fen Bilimleri Dergisi Part C: Tasarım ve Teknoloji, 8(4), 810-829.

Barewar, S. D., Tawri, S., Chougule, S. S. (2019). Heat transfer characteristics of free nanofluid jet on flat surface with different jet to plate distance: An experimental investigation. Chemical Engineering and Processing-Process Intensification, 136, 1-10.

Başaran, A., Selimefendigil, F. (2013). Numerical study of heat transfer due to twinjets impingement onto an isothermal moving plate. *Mathematical and Computational Applications*, *18*(3), 340-350.

Batchelor G. K.,(1977). " Effect of Brownian-Motion on bulk stress in a suspension of spherical-particles", Journal of Fluid Mechanics", vol.83(1), pp.97–117.

Boudraa, B., Bessaïh, R.(2020). Three-dimensional turbulent forced convection around a hot cubic block exposed to a cross-flow and an jet. *Heat Transfer*.

Buonomo, B., Manca, O., Bondareva, N. S., & Sheremet, M. A. (2019). Thermal and fluid dynamic behaviors of confined slot jets impinging on an isothermal moving surface with nanofluids. *Energies*, *12*(11), 2074.

Choi, S. U., Eastman, J. A. (1995). Enhancing thermal conductivity of fluids with nanoparticles (No. ANL/MSD/CP-84938; CONF-951135-29). Argonne National Lab., IL (United States).

Choo, K. S., Kim, S. J. (2010). Comparison of thermal characteristics of confined and unconfined impinging jets, School of Mechanical, Aerospace and System Engineering Korea Intsitute of Science and Technology, Sout Korea.

Corcione M.,(2011). "Empirical correlating equations for predicting the effective thermal conductivity and dynamic viscosity of nanofluids". Energy Conversion and Management, vol. 52(1), pp. 789–793.

Dagtekin, I., Oztop, H. F. (2008). Heat transfer due to double laminar slot jets impingement onto an isothermal wall within one side closed long duct. International communications in heat and mass transfer, 35(1), 65-75.

Devdatta, P.K., Debendra, K.D., Ravikanth S.V.,(2009). "Application of nanofluids in heating building and reducing pollution ", Applied Energy, vol.86, pp.2566-2573.

Dirlik, A.(2018), Nanokışkanlarda Doğal Taşınımla Isı Transferinin Sayısal Olarak İncelenmesi, (Master's thesis).

Elçioğlu, E. B. (2013). Experimental and theoretical investigations on alumina-water nanofluid viscosity with statistical analysis (Master's thesis).

Elçioğlu, E. B., Yazıcıoğlu, A.G., & Kakaç, S. (2014). Nanoakişkan Viskozitesinin Karşilaştirmali Değerlendirmesi. Isi Bilimi ve Teknigi Dergisi/Journal of Thermal Science & Technology, 34(1).

Elibol, E. A., Türkoğlu, H. (2017). Gözenekli Düz Bir Yüzeye Çarpan Jetin Sayısal Olarak İncelenmesi. Karadeniz Fen Bilimleri Dergisi, 7(1), 9-28.

Ersayın, E., Selimefendigil, F. (2013). Numerical investigation of impinging jets with nanofluids on a moving plate. *Mathematical and Computational Applications*, *18*(3), 428-437.

Etaig, S. (2017). Investigation of the enhancement of convective heat transfer for wall-bounded flows utilizing nanofluids (Doctoral dissertation, Northumbria University).

Feng, Y., Kleinstreuer, C.,(2010) " Nanofluid convective heat transfer in a parallel disk system", Int.J.Heat Mass Transfer, vol. 53(4), pp. 4619-4628.

Goharshadi E., K.Ahmadzadeh H., Samiiee S., Hadadian M., (2013).Nanofluids for heat transfer enhancement a review.

Hadad, K., Rahimian, A., Nematollahi, M.R.,(2013) " Numerical study of single and two phase models of water/Al2O3 nanofluid turbulent force convection flow in VVER-1000 nuclear reactor ", Ann. Nucl. Energy, vol.60, 287-294.

Ho, S.A., Hyungdae, K., Hanglin, J., Soon Ho, K., Wonpyo, C., Moo H.K.,(2010)" Experimental Study of Critical Heat Flux Enhancement during Forced Convective Flow Boiling of Nanofluid on a Short Heated Surface ", Int.J. Multiphase Flow, vol.36, 375-384.

Hofmann, H. M., Kind, M., Martin, H. (2007). Measurements on steady state heat transfer and flow structure and new correlations for heat and mass transfer in submerged jets. International Journal of Heat and Mass Transfer, 50(19-20), 3957-3965.

Hremya C., Miller S., Mallo T., Sinclai, J.,(1998) " Comparison of low Reynolds number k-ε turbulence models in predicting heat transfer rates for pipe flow, Int. J. Heat Mass Transfer. Vol 41 (11), 1543-1547.

Kakaç, S., Pramuanjaroenkıj, A. (2009). Review of convective heat transfer enhancement with nanofluids. International Journal of Heat and Mass Transfer, 52, 3187-3196.

Kareem, Z. S., Balla, H. H., AbdulWahid, A. F. (2019). Heat transfer enhancement in single circular impingement jet by CuO-water nanofluid. Case Studies in Thermal Engineering, 15, 100508.

Kasaeian, A., Eshghi, A.T., Sameti, M.,(2015) "A Review on The Applications of Nanofluids in Solar Energy Systems ", Renew. Sust. Energ. Rev., vol.43, pp.584-598.

Keblinski, P., Phillpot, S. R., Choi, S. U. S., Eastman, J. A. (2002). Mechanisms of heat flow in suspensions of nano-sized particles (nanofluids). International journal of heat and mass transfer, 45(4), 855-863.

Khan, I. A. (2021). Experimental validation of enhancement in thermal conductivity of titania/water nanofluid by the addition of silver nanoparticles. International Communications in Heat and Mass Transfer, 120, 104910.

Kilic M., Başkaya Ş.,(2017). Farklı geometride akış yönlendiriciler ve çarpan jet kullanarak yüksek ısı akılı bir yüzeyden olan ısı transferinin iyileştirilmesi, Journal of the Faculty of Engineering and Architecture of Gazi University, vol.32(3), pp.693-707.Web-1: 10.17341/gazimmfd.337616, 2017.

Kilic, M., Ozcan, O.,(2017). Numerical investigation of heat transfer and fluid flow of nanofluids with jets: International Conference On Advances and Innovations in Engineering (ICAIE); p.434-440.

Kilic, M. (2013). Çarpmalı Akışkan Jetlerle Kanal İçine Yerleştirilmiş Elemanlardan Olan Konveksiyonla Isı Transferinin Sayısal ve Deneysel Olarak İncelenmesi (Doktora Tezi, Gazi Üniversitesi, Fen Bilimleri Enstitüsü, Ankara).

Kilic, M., Ali, H. M. (2019). Numerical investigation of combined effect of nanofluids and multiple jets on heat transfer. Thermal Science, 23(5 Part B), 3165-3173.

Kilic, M., Çalışır, T. ve Başkaya, Ş.,(2017). "Experimental and numerical study of heat transfer from a heated flat plate in a rectangular channel with an Jet", Journal of the Brazilian Society of Mechanical Sciences and Engineering, vol.39(1), pp.329-344.

Kilic, M., Efeoğlu, M. (2019). Farklı parametreler için yüksek ısı akılı hareketli bir plakadan olan ısı transferinin sayısal incelenmesi. Çukurova 2nd International Multidisciplinary Studies Congress, Adana, Turkey, pp.355-364.

Kilic, M., Efeoğlu, M. (2019). Yüksek ısı akılı hareketli bir plakadan olan ısı transferinin farklı hacim oranları ve farklı tip nanoakışkanlar için incelenmesi. Çukurova 2nd International Multidisciplinary Studies Congress, Adana, Turkey, pp.345-354.

Kumar, P. M., Kumar, J., Tamilarasan, R., Sendhilnathan, S., Suresh, S. (2015). Review on nanofluids theoretical thermal conductivity models. Engineering Journal, 19(1), 67-83.

L., Xuan Y., Yu F.,(2012). " Experimental investigation of submerged single jet impingement using Cu-Water Nanofluid. Applied Thermal Engineering, vol.36 (1), pp.426–433.

Lahari, M. C., Sai, P. S. T., Swamy, K. N., KrishnaMurthy, N., Sharma, K. V. (2018, December). Investigation on heat transfer properties of water based TiO2-ZnO nanofluids. In IOP conference series: materials science and engineering (Vol. 455, No. 1, p. 012092).

Lee, S., Choi, S. S., Li, S. A., Eastman, J. A. (1999). Measuring thermal conductivity of fluids containing oxide nanoparticles.

Li, Y., Tung, S., Schneider, E., Xi, S. (2009). A review on development of nanofluid preparation and characterization. Powder Technology, 196(2), 89-101.

Lv J., Chang S., Hu C., Bai M., Wang P., Zeng K.(2017). " Experimental investigation of free single jet impingement using Al_2O_3 - water nanofluid ", International Communications in Heat and Mass Transfer, vol.88, pp.126–135.

McGuinn, A., Persoons, T., O'donovan T., Murray, D., (2007). Surface heat transfer from an synthetic air jet, International Journal of Heat and Mass Transfer", vol. 20, pp.1333-1338.

Medina, H. J. M. (2008). Study of Steady and Pulsating Jets (Doctoral dissertation, Ph. D. Dissertation, School of Mechanical and Aerospace Engineering, The Queen's University of Belfast, Belfast, United Kingdom).

Murshed S. M. S., Leong, K. C., Yang, C. (2005). Enhanced thermal conductivity of TiO_2 - water based nanofluids. International Journal of Thermal Sciences, 44**,** 367-373.

Murshed, S. M. S., Leong, K. C., Yang, C. (2008). Thermophysical and electrokinetic properties of nanofluids–a critical review. Applied Thermal Engineering, 28(17-18), 2109-2125.

Naraki, M., Peyghambarzadeh, S. M., Hashemabadi, S. H., Vermahmoudi, Y. (2013). Parametric study of overall heat transfer coefficient of CuO/water nanofluids in a car radiator. International Journal of Thermal Sciences, 66, 82-90.

Nayak, S.K., Mishra, P.C., Parashar, S.K.,(2016). " Enhancement of heat transfer by water – Al_2O_3 and water-TiO_2 nanofluids jet impingement in cooling hot surface steel surface", Journal of Experimental Nanoscience, vol.11, pp.1253-1273.

Nguyen, C. T., Desgranges, F., Galanis, N., Roy, G., Maré, T., Boucher, S., Mintsa, H. A. (2008). Viscosity data for Al_2O_3–water nanofluid—hysteresis: is heat transfer enhancement using nanofluids reliable? International journal of thermal sciences, 47(2), 103-111.

Nguyen, C. T., Galanis, N., Polidori, G., Fohanno, S., Popa, C. V., Le Bechec, A. (2009). An experimental study of a confined and submerged jet heat transfer using Al_2O_3-water nanofluid. International Journal of Thermal Sciences, 48(2), 401-411.

Özerinç, S. (2010). Heat transfer enhancement with nanofluids (Master's thesis, Middle East Technical University, Ankara)

Pak, B. C., Cho, Y. I.(1998) " Hydrodynamic and heat transfer study of dispersed fluids with submicron metallic oxide particles", Experimental Heat Transfer an International Journal, vol.11(2), pp.151–170.

Peyghambarzadeh, S. M., Hashemabadi, S. H., Hoseini, S. M., Jamnani, M. S. (2011). Experimental study of heat transfer enhancement using water/ethylene glycol based nanofluids as a new coolant for car radiators.International communications in heat and mass transfer, 38(9), 1283-1290.

Pordanjani, A. H., Aghakhani, S., Afrand, M., Mahmoudi, B., Mahian, O., Wongwises, S. (2019). An updated review on application of nanofluids in heat exchangers for saving energy. Energy Conversion and Management, 198, 111886.

Putra, N., Roetzel, W., Das, S. K. (2003). Natural convection of nano-fluids. Heat and mass transfer, 39(8), 775-784.

Riazi, H., Murphy, T., Webber, G. B., Atkin, R., Tehrani, S. S. M., & Taylor, R. A. (2016). Specific heat control of nanofluids: A critical review. International Journal of Thermal Sciences, 107, 25-38.

Sajid, M. U., Ali, H. M. (2018). Thermal conductivity of hybrid nanofluids: a critical review. International Journal of Heat and Mass Transfer, 126, 211-234.

Sarkar, J., Ghosh, P., Adil, A. (2015). A review on hybrid nanofluids: recent research, development and applications. Renewable and Sustainable Energy Reviews, 43, 164-177.

Selvakumar, P., Suresh, S.,(2012) "Convective Performance of CuO/Water Nanofluid in an Electronic Heat Sink, Exp., Thermal Fluid Science, vol. 40, 57-63.

Sharif, M. A. R., Banerjee, A. (2009). Numerical analysis of heat transfer due to confined slot-jet impingement on a moving plate. *Applied Thermal Engineering*, *29*(2-3), 532-540.

Sudarmadji, B. S. (2018). Performance Evaluation Criterion of Nanofluid. Microfluidics and Nanofluidics, 277.

Sun B., Qu Y., Yang D.,(2016) "Heat transfer of single jet with Cu nanofluids", Applied Thermal Engineering, vol. 102, pp. 701-707.

Sun, B., Guo, Y., Yang, D., Li, H. (2020). The effect of constant magnetic field on convective heat transfer of Fe_3O_4/water magnetic nanofluid in horizontal circular tubes. Applied Thermal Engineering, 171, 114920.

Sun, B., Zhang, Y., Yang, D., Li, H. (2019). Experimental study on heat transfer characteristics of hybrid nanofluid jets. Applied Thermal Engineering, 151, 556-566.

Sundar, L. S., Singh, M. K., & Sousa, A. C. (2013). Thermal conductivity of ethylene glycol and water mixture based Fe_3O_4 nanofluid. International communications in heat and mass transfer, 49, 17-24.

Suresh, S., Chandrasekar, S., Sekhar, C.,(2011) "Experimental Studies on Heat Transfer and Friction Factor Characteristics of CuO/Water Nanofluid under Turbulent Flow in a Helically Dimpled Tube", Exp.Thermal Fluid Sci., vol.35, pp.542-549.

Teamah, M.A., Dawood, M.M., Shehata, A.,(2015) "Numerical and experimental investigation of flow structure and behavior of Nanofluids flow impingement on horizontal flat plate ", Experimental Thermal and Fluid Science, vol.74, 235-246.

Timofeeva, E. V., Moravek, M. R., Singh, D. (2011). Improving the heat transfer efficiency of synthetic oil with silica nanoparticles. Journal of colloid and interface science, 364(1), 71-79.

Umer A., Naveed S., Ramzan N.,(2015) " Experimental study of laminar forced convection heat transfer of deionized water based copper (I) oxide nanaofluids in tube with constant wall heat flux", Heat Mass Transfer, vol.52, pp.2015-2025.

Wang B.X., Zhou L.P., Peng X.F.(2006) " Surface and size effects on the specific heat capacity of nanoparticles", International Journal of Thermophysics, vol.27(1), pp.139–151.

Wang, B., Zhou, L., and Peng, X., (2003), “A Fractal Model for Predicting the Effective Thermal Conductivity of Liquid with Suspension of Nanoparticles,” Int. J. Heat Mass Tran., 46(14), pp. 2665-2672.

Xuan, Y., Li, Q. (2000). Heat transfer enhancement of nanofluids. International Journal of Heat and fluid flow, 21(1), 58-64.

Zhang, J., Diao, Y., Zhao, Y., & Zhang, Y. (2014). Experimental study of TiO_2–water nanofluid flow and heat transfer characteristics in a multiport minichannel flat tube. International Journal of Heat and Mass Transfer, 79, 628-638.

App. 1. CFD flow diagram